Epigenetic transitions leading to heritable, RNA-mediated de novo silencing in *Arabidopsis thaliana*

Donna M. Bond and David C. Baulcombe[1]

Department of Plant Sciences, University of Cambridge, Cambridge CB2 3EA, United Kingdom

Edited by Steven E. Jacobsen, University of California, Los Angeles, CA, and approved November 18, 2014 (received for review July 10, 2014)

In plants, RNA-directed DNA methylation (RdDM), a mechanism where epigenetic modifiers are guided to target loci by small RNAs, plays a major role in silencing of transposable elements (TEs) to maintain genome integrity. So far, two RdDM pathways have been identified: RNA Polymerase IV (PolIV)-RdDM and RNA-dependent RNA Polymerase 6 (RDR6)-RdDM. PolIV-RdDM involves a self-reinforcing feedback mechanism that maintains TE silencing, but cannot explain how epigenetic silencing is first initiated. A function of RDR6-RdDM is to reestablish epigenetic silencing of active TEs, but it is unknown if this pathway can induce DNA methylation at naïve, non-TE loci. To investigate de novo establishment of RdDM, we have used virus-induced gene silencing (VIGS) of an active *FLOWERING WAGENINGEN* epiallele. Using genetic mutants we show that unlike PolIV-RdDM, but like RDR6-RdDM, establishment of VIGS-mediated RdDM requires PolV and DRM2 but not Dicer like-3 and other PolIV pathway components. DNA methylation in VIGS is likely initiated by a process guided by virus-derived small (s) RNAs that are 21/22-nt in length and reinforced or maintained by 24-nt sRNAs. We demonstrate that VIGS-RdDM as a tool for gene silencing can be enhanced by use of mutant plants with increased production of 24-nt sRNAs to reinforce the level of RdDM.

RNA-directed DNA methylation | virus-induced gene silencing | epigenetics | *Arabidopsis thaliana*

Methylation of cytosine (C) residues of DNA is a stable and heritable modification that mediates epigenetic control in eukaryotic genomes. In plants this modification occurs at CG, CHG, and CHH sequences (where H can be C, A, or T) and involves RNA-directed DNA methylation (RdDM) pathways. The DNA methyltransferases in these pathways are guided to target loci by ribonucleoproteins in which a small (s)RNA is the specificity determinant (1, 2).

There are two mechanisms to maintain DNA methylation. In RdDM pathways acting at predominantly transposable elements (TEs), SAWADEE HOMEODOMAIN HOMOLOG (SHH)1 binds and recruits RNA Polymerase IV (PolIV) to transcribe methylated DNA (3, 4). The PolIV transcripts are then made double-stranded by RNA-dependent RNA polymerase (RDR)2 and cleaved by Dicer-like 3 (DCL3) into 24-nt sRNAs that are loaded into and guide AGONAUTE (AGO)4 to complementary scaffold RNAs transcribed from the same locus by RNA polymerase V (PolV). The sRNA-bound AGO and the PolV transcript interact and recruit the de novo methyltransferase DRM2 that modifies C residues of the DNA strand acting as the template for PolV (5).

Maintenance of CG and CHG methylation during DNA replication occurs via MET1, the plant homolog of the mammalian DNA methyltransferase DNMT1, and the plant-specific CHROMOMETHYLASE 3 (CMT3) that works in concert with the SU(VAR)3-9 HOMOLOG (SUVH) SET domain histone methyltransferse KRYPTONITE. Both MET1 and CMT3 act independently of sRNAs but maintenance of CHH methylation within euchromatin is dependent on the continuous operation of the sRNA establishment mechanism, resulting in a self-reinforcing loop (1). This PolIV-RdDM maintenance step is stabilized by SHH1 and the SUVH2/9 SET domain proteins, which bind methylated DNA and continue to recruit PolIV and PolV, respectively to RdDM sites (3, 4, 6, 7). Maintenance of CHH methylation within heterochromatin involves CMT2 and relies on repressive chromatin modifications, independent of sRNAs (8, 9).

The detailed analyses of PolIV-RdDM provide a good explanation of how methylated Cs in an asymmetric context (CHH) can be maintained through feedback mechanisms, but they do not explain how DNA methylation at naïve loci can be first established. A second RdDM pathway has been proposed in which the sRNAs are 21/22-nt rather than 24-nt in length and PolIV is not involved (10–12). This process is referred to as RDR6-RdDM to reflect the identity of the required RDR ortholog in *Arabidopsis*, and it was hypothesized that, in connection with the silencing of TEs and DNA methylation at trans-acting-siRNA (tasiRNA) loci, posttranscriptional gene silencing (PTGS) of PolII-derived transcripts is the trigger. However, the analysis of this mechanism did not conclusively demonstrate a role in RNA-mediated de novo silencing, and the establishment and maintenance phases of silencing at these loci cannot be easily distinguished.

To further investigate the de novo establishment of DNA methylation in plants we infected transgenic plants expressing a GFP transgene with an RNA virus carrying the promoter sequence of the reporter gene (13). On infection, the plant's antiviral defense mechanism produced sRNAs against the virus and the promoter through virus-induced gene silencing (VIGS) (14). The reporter gene was silenced in the infected plant because of increased DNA methylation at its promoter that was maintained in later generations when the virus was no longer present. It was presumed that, like heritable silencing of TEs, the RdDM pathway

Significance

Using virus-induced gene silencing (VIGS) in wild-type and mutant *Arabidopsis*, we characterize a novel mechanism associated with the de novo establishment of heritable epigenetic marks in plants. Once established by this novel mechanism, the epigenetic mark is then reinforced by the previously characterized PolIV pathway of RNA-directed DNA methylation. A similar transition from the novel mechanism to the PolIV pathway is likely to explain many epigenetic phenomena in which RNA-directed DNA methylation is established de novo, including transposon silencing and paramutation. A practical benefit of our work is the identification of a mutant plant genotype in which the maintenance mechanism of epigenetic VIGS is reinforced. This genotype would aid the use of epigenetic VIGS for dissection of gene structure and function.

Author contributions: D.M.B. and D.C.B. designed research; D.M.B. performed research; D.M.B. and D.C.B. analyzed data; and D.M.B. and D.C.B. wrote the paper.

The authors declare no conflict of interest.

This article is a PNAS Direct Submission.

Freely available online through the PNAS open access option.

Data deposition: The sequence reported in this paper has been deposited in the Array Express database, www.ebi.ac.uk/arrayexpress (accession no. E-MTAB-3009).

[1]To whom correspondence should be addressed. Email: dcb40@cam.ac.uk.

This article contains supporting information online at www.pnas.org/lookup/suppl/doi:10.1073/pnas.1413053112/-/DCSupplemental.

was responsible for the establishment of VIGS-RdDM. However, these experiments in *Nicotiana benthamiana* could not test for involvement of pathways that had been previously characterized in *Arabidopsis*.

Using VIGS in *Arabidopsis*, we show that sRNAs can initiate heritable DNA methylation and transcriptional gene silencing (TGS) at an endogenous locus. The virus-derived sRNAs responsible for establishing DNA methylation are likely to be 21/22-nt in length and establishment occurs without canonical PolIV-RdDM, but requires PolV and DRM2. An earlier initiation stage of RNA-mediated de novo silencing may occur independently of DNA methylation. Furthermore, mutant plants producing highly abundant 24-nt sRNAs exhibit reinforced maintenance of RdDM. From our results with VIGS-RdDM, we propose three steps for de novo, heritable DNA methylation at endogenous loci in plants—initiation, establishment, and maintenance—which can occur with or without the presence of 24-nt sRNAs.

Results

VIGS of *FLOWERING WAGENINGEN*. To test the involvement of the PolIV-RdDM pathway in the establishment of DNA methylation, we set up a VIGS system in *Arabidopsis thaliana*. Our strategy was to first characterize VIGS in wild-type plants and then to test RNA silencing mutants for effects on epigenetic silencing of an endogenous target locus. We used tobacco rattle virus (TRV) as the viral vector (15, 16) and an active *FLOWERING WAGENINGEN* (*FWA*) epiallele, in the *fwa-d* epimutant (17), as the target locus. Most of the analyses described here involved plants carrying this epiallele, although for some comparative analyses the plants were wild-type Columbia (Col-0) carrying a naturally silenced allele of *FWA* (18). We refer to the two different epigenotypes as Col-0(FWA^{C}) and Col-0(FWA^{Cme}), respectively, to reflect the status of C methylation at *FWA*.

One TRV construct (TRV:FWAtr) included the direct tandem repeats from the *FWA* promoter and transcribed sequence extending to the second intron within the 5′UTR, a region previously shown to be required for silencing of *FWA* (17, 19). This construct was designed to test epigenetic silencing mechanisms. A second construct, to investigate PTGS, carried part of the *FWA* coding sequence (TRV:FWAcds) (Fig. S1 *A* and *B*).

In the infected plants (V_0 generation) the level of *FWA* sRNAs correlated with the levels of viral RNA (Fig. 1 *A* and *B*) and, with TRV:FWAcds, the *FWA* mRNA was correspondingly less abundant than in control plants. Some repression of *FWA* mRNA was evident in plants infected with TRV:FWAtr, but the level of silencing did not correlate with the level of virus and by 45 d post-infection (dpi) it returned to levels in mock-infected plants (Fig. 1*C* and Fig. S1 *C* and *D*). From these data we conclude that effective posttranscriptional but not epigenetic silencing of *FWA* could be triggered by these TRV VIGS constructs. However, the TRV:FWAcds-infected plants did not flower early (Fig. S1*E*), as would be expected from the reduced expression of *FWA*. This lack of phenotype is most likely because the silencing was too weak or because early flowering was repressed by FWA that had been produced before virus inoculation (20).

The lack of epigenetic VIGS with TRV:FWAtr could indicate that the target promoter sequence was refractory to silencing or that epigenetic silencing was restricted to one allele and was masked by the expressed second allele. To test the second scenario we investigated the flowering time of progeny of TRV:FWAtr-infected plants (V_1 generation) in the expectation that some plants might have inherited two silenced alleles of *FWA*, as in transgene-induced *FWA* silencing (17, 19). Many of the V_1 plants flowered late, as did the Col-0(FWA^{C}) controls. However, in the progeny of TRV:FWAtr- but not TRV- or TRV:FWAcds-infected plants, there were individuals that flowered as early as Col-0(FWA^{Cme}) plants with fully silenced *FWA* (Fig. 1*D* and Fig. S2 *A* and *B*). The proportion of early flowering plants did not follow a simple 1:3 ratio, as would be expected if heterozygous epialleles in the V_0 plant were stably inherited: it was either more or less than 1:3. We conclude that *FWA* silencing affected

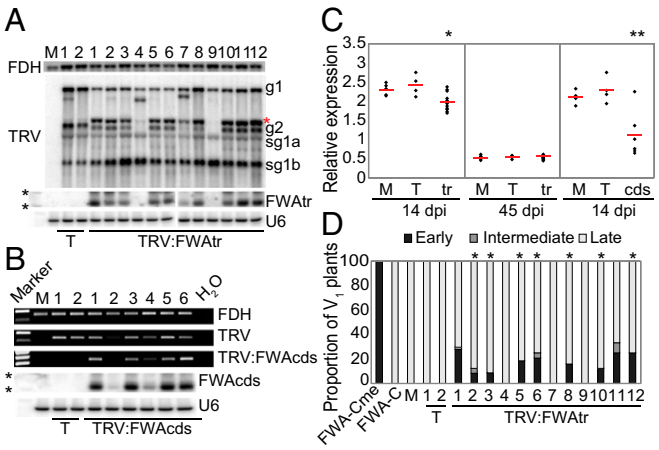

Fig. 1. Establishing VIGS of *FWA*. (*A*, *Upper*) Northern blot with TRV RNA species (Fig. S1*B*) and (*Lower*) sRNA Northern blot with *FWAtr* sRNAs in TRV:FWAtr-, TRV (T)-, or mock (M)-infected Col-0(FWA^{C}) plants, 14 dpi. *FDH* and *U6* were probed as loading controls, respectively. TRV:FWAtr is marked with a red asterisk. The black asterisks represent the 20-nt and 30-nt sRNA markers. For the sRNA Northern blot analysis, TRV:FWAtr-infected samples 7–12 were run on a separate gel as indicated by the white separating line between samples 6 and 7. (*B*, *Upper*) RT-PCR of TRV and TRV:FWAcds in TRV:FWAcds-, TRV (T)-, or mock (M)-infected Col-0(FWA^{C}) plants, 14 dpi. *FDH* was assayed as an internal control. (*Lower*) sRNA Northern blot with *FWAcds* sRNAs in the same plants. *U6* was probed as a loading control. The black asterisks represent the 20-nt and 30-nt sRNA markers. (*C*) *FWA* expression in TRV:FWAtr- (tr), TRV:FWAcds- (cds), TRV- (T), or mock (M)-infected Col-0 (FWA^{C}) plants, 14 dpi and 45 dpi. Each sample is represented by a black diamond and the average of all samples per treatment is represented by the red horizontal line. A two-tailed Student *t* test suggested *FWA* expression was repressed by TRV:FWAtr (*$P < 0.05$) and TRV:FWAcds (**$P < 0.01$), 14dpi. (*D*) Proportion of early- (black), intermediate- (dark gray), and late- (light gray) flowering V_1 progeny from TRV:FWAtr-, TRV (T)-, or mock (M)-infected Col-0(FWA^{C}) plants (*A*), compared with Col-0(FWA^{Cme}) and Col-0(FWA^{C}). Lines with a ratio of <1 (early):3 (late) are marked with a black asterisk.

both alleles but that effects were not seen in the infected plant because they were initially weak and became progressively stronger during the transition between generations. Similar results were obtained with VIGS of the unsilenced *fwa-2* epimutant (18) in the Ler background (Fig. S2*C*).

The progressive silencing of *FWA* was not a result of persistence of TRV:FWAtr because we failed to detect virus in ∼200 tested early flowering progeny using a PCR test (*SI Materials and Methods*). It was likely therefore that silencing was initiated in the V_0 plant without affecting expression of *FWA*. The silencing of this gene would then have been established more completely in the transition between generations, or in the V_1 plants. The proportion of early-flowering V_1 progeny correlated positively with the level of virus infection and *FWAtr* sRNAs in the parent plant, consistent with initiation of epigenetic silencing in the infected plants (compare Fig. 1*A* with Fig. 1*D*).

The early-flowering time in the V_1 progeny of infected plants was associated with changes in DNA methylation at the TRV:FWAtr target site (*FWAtr*). The *FWAtr* DNA in leaf or floral tissue from V_0 plants was not methylated (Fig. S1*F*), but in the V_1 progeny it was hypermethylated at levels similar to those in Col-0(FWA^{Cme}) plants (Fig. 2*A*). Hypermethylation was established in all C sequence contexts (Fig. 2*B*) and, in the earliest flowering V_1 plants, CHH methylation was 10–20% higher than wild-type Col-0(FWA^{Cme}) with naturally silenced *FWA*. In V_1 plants with an intermediate-flowering time the degree of methylation at *FWA* was 20–40% less than in early-flowering plants, although the proportion of methylated C residues in the CHH context was 20–50%: two to five times more than in Col-0 (FWA^{Cme}) (Fig. 2*B* and Fig. S2*D*). Most of this intermediate DNA methylation was at the 5′ end of the TRV:FWAtr target

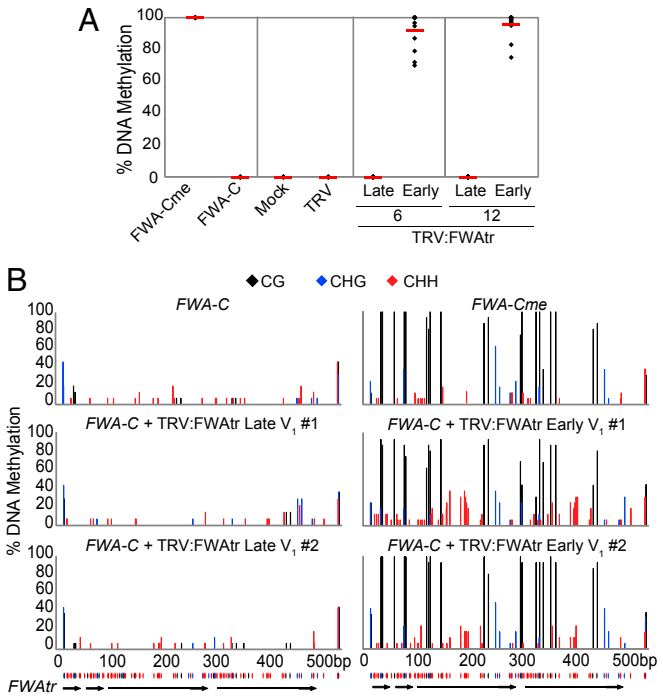

Fig. 2. VIGS-RdDM of *FWA* induces early flowering in V_1 progeny plants. (*A*) DNA methylation (McrBC-qPCR) at *FWAtr* in V_1 progeny of Col-0(FWA^C) plants infected with TRV:FWAtr, TRV, or mock conditions compared with Col-0(FWA^{Cme}) and Col-0(FWA^C) plants. DNA from early- and late-flowering progeny from TRV:FWAtr-infected lines 6 and 12 (Fig. 1*A*) were assayed. Each independent sample is represented by a black diamond and the average of all samples per treatment is represented by the red horizontal line. (*B*) Bisulfite sequencing analysis of DNA methylation at *FWAtr* in early- and late-flowering V_1 progeny plants from *A*. Col-0(FWA^{Cme}) and Col-0(FWA^C) were included as a comparison. The position of C residues along the *FWAtr* region (black arrows) is represented by the ticks on the *x* axis and the context of methylation is represented by the different colors: CG is in black, CHG is in blue, and CHH is in red.

region (Fig. S2*D*), suggesting that VIGS-RdDM was established at the 5′ end of the tandem repeats and that it then spread in the 5′→3′ direction.

Flowering time and DNA methylation at *FWA* cosegregate in a Mendelian ratio in an F_2 population produced from a cross between plants with *FWA* in a silent (FWA^{Cme}) and active (FWA^C) state (18). In contrast, consistent with a progressive increase in *FWA* silencing between generations, the V_2 progeny of intermediate-flowering V_1 plants all gained DNA methylation at *FWA* and flowered at the same time as Col-0(FWA^{Cme}) (Fig. S3 *A* and *B*). This progressive silencing, together with the complete transmission of the *FWA* silenced and hypermethylated phenotype to the V_2 generation from the early-flowering V_1 plants (Fig. S3), indicates that TRV:FWAtr infection leads to transgenerational epigenetic silencing of the *FWA* promoter sequence, as with the original TRV:35S system (13). However, unlike the TRV:35S system, we could not detect the epigenetic silencing in the infected plants (Fig. S1*F*). To explain the *FWA* silencing in the V_1 generation we propose that establishment of the epigenetic mark involved cryptic epigenetic changes to the *FWAtr* sequence in the infected plant. In the following sections we first describe a genetic analysis of *FWA* promoter VIGS and, second, a further analysis of establishment.

Separate RdDM Pathways for CG and CHH Methylation. To investigate the genetic requirements for *FWA* promoter VIGS, we infected FWA^C plants that carried mutations in various genes known to act in PolIV-RdDM (Table S1). Inoculation was with TRV:FWAtr, TRV, or mock conditions (Fig. S4*A*) and, as with the Col-0(FWA^C), there was no change in flowering time of the V_0 plants in any of the mutant backgrounds (Fig. S4*B*).

In the V_1 progeny of infected *poliv*(FWA^C), *rdr2*(FWA^C), *dcl3* (FWA^C), and *ago4*(FWA^C) genotypes, as with Col-0(FWA^C), there were early- and intermediate-flowering plants (Fig. 3*A* and Fig. S5) that gained DNA methylation at *FWAtr* (Fig. 3*B* and Fig. S6*A*). However, the RdDM in all instances with these mutants was predominantly in a CG context and, in the intermediate plants, it was restricted to the 5′ end of the tandem repeat (Fig. S6*B*). In contrast, none of the V_1 progeny of *polv*(FWA^C)- or *drm1/2*(FWA^C)-infected plants were early flowering. From these data we conclude that there are at least two mechanisms involved in RdDM. First, there is a PolIV-, RDR2-, DCL3-, and AGO4-independent process leading to RdDM of C residues in a CG or CHG context. This process is clearly sufficient for silencing of *FWA*. A second process is dependent on PolIV, RDR2, DCL3, AGO4, PolV, and DRM2, and it affects CHH methylation.

In addition to DCL3, *Arabidopsis* encodes DCL1, -2, and -4 that generate 21-nt miRNAs, 22-nt sRNAs, and 21-nt sRNAs, respectively (21) and, in a separate assay for *FWA* silencing, there was a redundant requirement of DCL proteins (22). To further explore the DCL requirement in VIGS-RdDM, we assessed the *dcl2*(FWA^C), *dcl4*(FWA^C), *dcl2/4*(FWA^C), and *dcl2/3/4*(FWA^C) mutants in our assay. The viral load in *dcl2/4*(FWA^C) and *dcl2/3/4*(FWA^C) V_0 plants was much greater than Col-0 (FWA^C) plants (Fig. S4*C*), consistent with the role of DCL2 and DCL4 acting in the antiviral RNA silencing pathway (23). The proportion of early-flowering V_1 progeny from

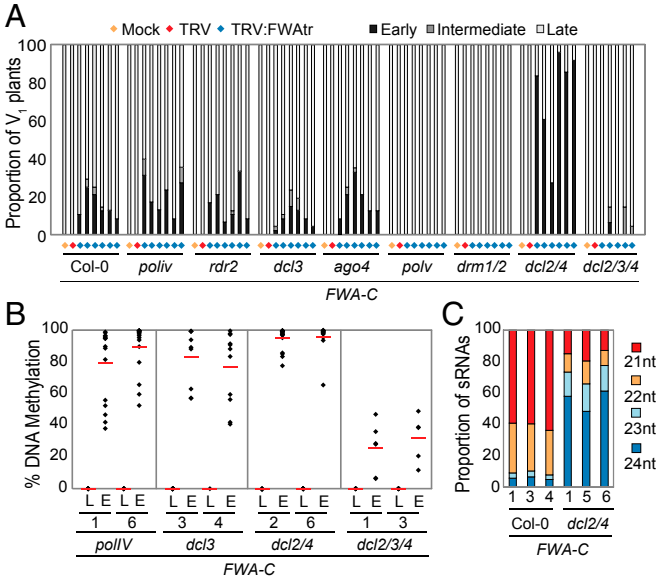

Fig. 3. VIGS-RdDM of *FWA* requires PolV and DRM2 and is enhanced in a *dcl2/4* mutant. (*A*) Proportion of early- (black), intermediate- (dark gray), and late- (light gray) flowering V_1 progeny from Col-0(FWA^C), *poliv*(FWA^C), *rdr2*(FWA^C), *dcl3*(FWA^C), *ago4*(FWA^C), *polv*(FWA^C), *drm1/2*(FWA^C), *dcl2/4* (FWA^C), and *dcl2/3/4*(FWA^C) mutants infected with TRV:FWAtr (blue diamond), TRV (red diamond), or mock (orange diamond) conditions. (*B*) DNA methylation (McrBC-qPCR) at *FWAtr* in early- (E) and late- (L) flowering V_1 progeny from two independent lines of *poliv*(FWA^C), *dcl3*(FWA^C), *dcl2/4* (FWA^C), and *dcl2/3/4*(FWA^C) mutants. Each independent sample is represented by a black diamond and the average of all samples per treatment is represented by the red horizontal line. (*C*) Proportion of different size classes of sRNAs that map to *FWAtr* in Col-0(FWA^C) and *dcl2/4*(FWA^C) TRV:FWAtr-infected V_0 plants. The proportion of 21-nt (red), 22-nt (orange), 23-nt (light blue), and 24-nt (dark blue) sRNA reads was determined from the actual read count, corrected for multiple mapping. Three independent samples per genotype were assessed (Fig. S4 *A* and *C*).

TRV:FWAtr-infected *dcl2*(*FWA*^{C}) and *dcl4*(*FWA*^{C}) plants was similar to Col-0(*FWA*^{C}), but there were many more early-flowering V_1 progeny from *dcl2/4*(*FWA*^{C}) plants (Fig. 3*A* and Fig. S5). For some lines almost 100% of V_1 progeny flowered early and, correspondingly, there was a high degree of DNA methylation at *FWAtr* in these plants (Fig. 3*B* and Fig. S6*A*). This *FWAtr* hypermethylation in *dcl2/4*(*FWA*^{C})-infected plants was more biased to the CG context than with the VIGS of Col-0(*FWA*^{C}) plants.

In the TRV:FWAtr-infected *dcl2/4*(*FWA*^{C}) V_0 plants, unlike the wild-type plants, repression of *FWA* correlated with DNA methylation at *FWAtr* (10–50%) (Fig. S4 *D*–*G*). In a minority of plants, *FWA* was repressed independent of DNA methylation, suggesting PTGS of *FWA* may precede TGS, or an alternative repressive epigenetic mark could be present at *FWA* before initiation of DNA methylation. The pattern of DNA methylation established in the *dcl2/4*(*FWA*^{C}) V_0-infected plants was in all sequence contexts, with increased levels of CHH methylation presumably because of the high level of 24-nt sRNAs in these plants (Fig. S4*A*). However, deep sequencing of sRNAs from TRV:FWAtr-infected *dcl2/4*(*FWA*^{C}) V_0 plants indicated that ~22–35% of sRNAs mapping to the *FWAtr* target region are 21/22-nt in length (compared with 90% in wild-type) (Fig. 3*C* and Fig. S7), consistent with the possibility that 21/22-nt sRNAs play a role in the establishment of DNA methylation in this system.

In contrast, the RdDM and *FWA* silencing in the V_1 progeny of infected *dcl2/3/4*(*FWA*^{C}) plants was not enhanced. TRV:FWAtr infection triggered early or intermediate flowering in a minority of the V_1 generation plants (Fig. 3*A* and Fig. S5) and, overall, the level of DNA methylation, predominantly in the CG context, was less than in the V_1 progeny of Col-0(*FWA*^{C}) plants (Fig. 3*B* and Fig. S6*A*). This finding indicates that the greater silencing of *FWA* in *dcl2/4*(*FWA*^{C}) V_1 plants was dependent on DCL3, and consistent with this interpretation there were abundant 24-nt *FWAtr* sRNAs in the infected *dcl2/4*(*FWA*^{C}) plants (Fig. 3C and Figs. S4*A* and S7). In *dcl2/3/4*(*FWA*^{C}) V_0 plants there were only a low abundance of 21/22-nt *FWAtr* sRNAs (Fig. S4*A*), despite comparable levels of viral load in infected *dcl2/4* (*FWA*^{C}) and *dcl2/3/4*(*FWA*^{C}) mutants (Fig. S4*C*). However, because *FWA* silencing was not eliminated in the V_1 progeny of *dcl2/3/4*(*FWA*^{C}) plants, the epigenetic silencing of *FWA* must have been initiated and established in the absence of DCL3 as with the V_1 progeny of the *dcl3*(*FWA*^{C}) mutant.

Establishment of *FWA* Epigenetic Silencing. To further investigate the establishment step in VIGS-RdDM of *FWA* we made reciprocal crosses between mock-infected and TRV:FWAtr-infected Col-0(*FWA*^{C}) plants (Fig. S8*A*) and analyzed the flowering time of the F_1 progeny. Most of these F_1 plants flowered late, indicating that *FWA* was not silenced. However, F_1 progeny from 15 of 61 lines tested had an intermediate flowering time phenotype (irrespective of the direction of the cross) and had ~50% DNA methylation at *FWAtr* (Fig. 4 and Fig. S8 *B* and *C*). Furthermore, the flowering-time behavior of self-fertilized F_2 populations from the intermediate F_1 plants segregated in a 1:2:1 (early:intermediate:late) ratio (Fig. S8*D*). We conclude from these data that the methylated allele in F_1 plants was inherited from the TRV:FWAtr-infected parent, consistent with the semidominant mutation of *FWA* (18), and that this silent state was not transmitted to the allele from the mock-infected plant. The initiation of *FWA* silencing must have occurred at the DNA or chromatin level in the V_0 plant and these data rule out that a transacting initiating factor, for example an RNA, is transmitted from the infected plant into its progeny.

The early-flowering phenotype was an infrequent characteristic in V_1 progeny of Col-0(*FWA*^{C})-infected plants (185 of 1,061; progeny from 27 TRV:FWAtr-infected lines presented here). However, the *FWA* DNA of all early-flowering V_1 plants was either fully methylated or became fully methylated in the V_2 generation (Fig. S3), suggesting that both gametes had undergone an epigenetic conversion in the V_0 plant that would be manifested as full DNA methylation in the V_1 or V_2 plants. It

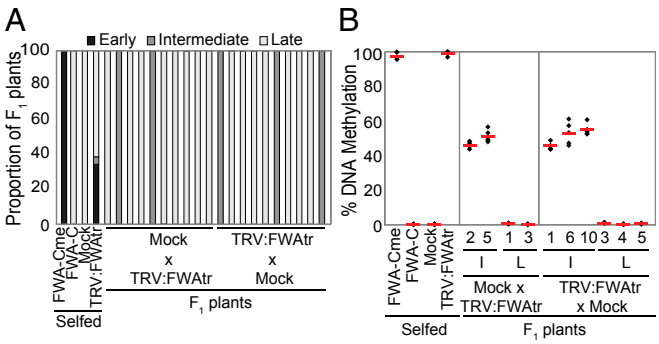

Fig. 4. VIGS-RdDM at *FWA* is established before or during gametogenesis. (*A*) Proportion of early- (black), intermediate- (dark gray), and late- (light gray) flowering F_1 progeny from reciprocal crosses between mock- and TRV:FWAtr-infected Col-0(*FWA*^{C}) plants, compared with self-fertilized Col-0 (*FWA*^{Cme}), Col-0(*FWA*^{C}), mock-, and TRV:FWAtr-infected Col-0(*FWA*^{C}) plants. (*B*) DNA methylation (McrBC-qPCR) at *FWAtr* in intermediate- (I) and late- (L) flowering F_1 progeny from reciprocal crosses between mock- and TRV:FWAtr-infected Col-0(*FWA*^{C}) plants (*A*), compared with self-fertilized control plants. Each independent sample is represented by a black diamond and the average of all samples per treatment is represented by the red horizontal line.

must be, therefore, that the infrequent epigenetic conversion in the infected plant affects either both *FWA* alleles or none. To test this hypothesis, we harvested individual siliques from Col-0 (*FWA*^{C}) V_0 plants infected with TRV:FWAtr (Fig. S8*A*) and measured the flowering time of the individual progeny. We found that most individual siliques produced 100% late-flowering progeny (Fig. S8*E*), consistent with the low frequency of early-flowering behavior transmitted to the V_1 progeny. However, there were some rare siliques with 50–100% of seed that grew into early-flowering plants. The concentration of *FWA* silencing in a few siliques further supports that an epigenetic factor is inherited through both gametes within certain flowers of the infected plant.

To further investigate when silencing of *FWA* is initiated, we assessed the degree of DNA methylation at *FWAtr* in a population of pollen cells from V_0 plants. In Col-0(*FWA*^{Cme}) plants, the *FWA* tandem repeat is demethylated at certain C residues within the vegetative nucleus (VN) of pollen because of the action of the DNA glycosylase DEMETER (DME), but full *FWAtr* DNA methylation is maintained in the sperm cells (SC) (24, 25). Therefore, on average 66% of DNA from pollen of a Col-0 (*FWA*^{Cme}) plant will be fully methylated at *FWAtr*. We predict if *FWA* silencing is initiated in the gametes or earlier, a proportion of pollen SCs from TRV:FWAtr-infected Col-0(*FWA*^{C}) plants will be fully methylated like Col-0(*FWA*^{Cme}).

To test this hypothesis, we bisulfite-sequenced pollen DNA from mock- and TRV:FWAtr-infected Col-0(*FWA*^{C}) (Fig. S8*A*) and *dcl2/4*(*FWA*^{C}) (Fig. S4*D*) plants and compared this to Col-0 (*FWA*^{Cme}) and *dcl2/4*(*FWA*^{Cme}) plants (Fig. 5 and Fig. S9 *A* and *B*). Approximately 20% of clones representing Col-0(*FWA*^{Cme}) and *dcl2/4*(*FWA*^{Cme}) DNA lacked C methylation at residues that are demethylated in the VN (24). This value is consistent with bisulfite sequencing clones representing DNA from SC and the VN, although the proportion of unmethylated DNA is lower than the predicted 33%. The deviation is likely a result of preferential amplification of methylated DNA in the PCR.

No clones of pollen DNA from Col-0(*FWA*^{C}) and *dcl2/4* (*FWA*^{C}) mock-infected plants contained methylated Cs at *FWAtr*. In contrast, 10–25% of clones representing pollen DNA from Col-0 (*FWA*^{C}) TRV:FWAtr-infected plants were methylated in all sequence contexts at the *FWA* target (Fig. 5*A* and Fig. S9*A*). Because of this small sample size, we are unable to differentiate DNA from the SC and VN with confidence, but the presence of fully methylated clones indicates that DNA from SC is represented. Consistent with this interpretation is the correlation of DNA methylation in pollen of TRV:FWAtr-infected Col-0(*FWA*^{C})

plants with the proportion of early-flowering progeny (Fig. S9*C*). This correlation was most striking in samples from *dcl2/4* (*FWA*^{C})-infected plants in which 80–85% of pollen DNA was methylated (Fig. 5*B* and Fig. S9*B*), corresponding to highly abundant early-flowering V_1 progeny (Fig. 3*A* and Fig. S9*D*). From these results we conclude that VIGS-RdDM of *FWA* in TRV:FWAtr-infected plants takes place either at or before gametogenesis.

Discussion

Epigenetic Transitions in de Novo Silencing. Our analysis of *FWA* promoter VIGS was based on the expectation that the canonical PolIV-RdDM pathway would be involved in establishing heritable silencing in the infected plants. In subsequent generations we anticipated that, as with 35S promoter VIGS in *N. benthamiana*, persistence of heritable epigenetic marks would be independent of RNA and dependent on the maintenance methyltransferase, MET1 (13). However, our data are not consistent with that prediction. The data indicate instead that heritable silencing of *FWA* involves a complex sequence of epigenetic transitions in which the canonical PolIV-RdDM pathway is involved but not essential. We propose below that the same sequence of epigenetic transitions applies generally when epigenetic marks in plants are established de novo by an RNA-based mechanism.

Our conclusions are based primarily on two key findings. First there is the unexpected observation that *FWA* promoter VIGS in wild-type plants is largely independent of key components of PolIV-RdDM, including PolIV, RDR2, DCL3, and AGO4 (Fig. 3 and Fig. S6). This finding prompts a radical shift from previous views about RdDM in which most of these proteins were viewed as necessary for establishment of DNA methylation (1, 2).

The second key finding with *FWA* promoter VIGS, unlike 35S promoter VIGS, was that the epigenetic silencing could be established without detectable effect in the V_0 plant and is progressively reinforced over two or three generations. The progression was associated eventually with DNA methylation in CG, CHG, and CHH contexts that spread from the 5′ to the 3′ part of the promoter relative to the direction of transcription (Fig. S2*D*). Consistent with this observation, sRNAs mapped primarily to the 5′ end of *FWAtr* in Col-0(*FWA*^{C}) and *dcl2/4*(*FWA*^{C}) TRV:FWAtr-infected V_0 plants (Fig. S7).

We discuss below how the slow progression of silencing in the *FWA* promoter VIGS system allowed resolution of the epigenetic transitions, including establishment and partially redundant systems for maintenance that is either dependent or independent of RNA. The transitions were less apparent with 35S promoter VIGS because it segued rapidly from establishment in the infected plant into RNA-independent maintenance in the progeny.

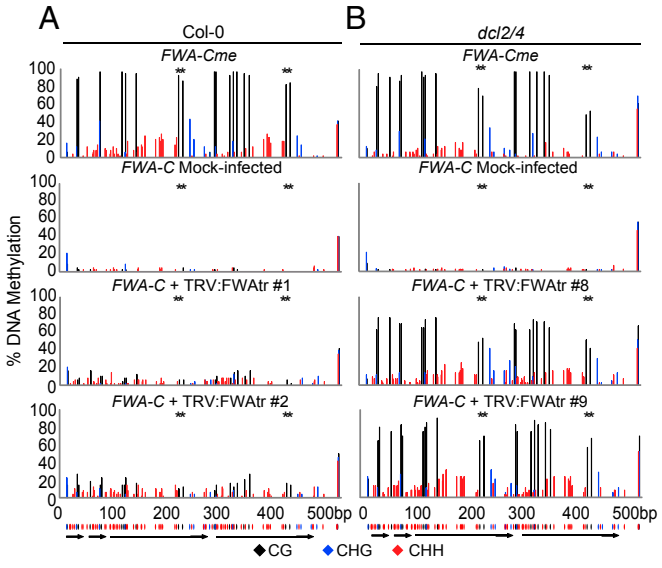

Fig. 5. *FWAtr* is methylated in pollen of TRV:FWAtr-infected plants. Bisulfite sequencing analysis of DNA methylation at *FWAtr* in pollen from mock- and TRV:FWAtr-infected (*A*) Col-0(*FWA*^{C}) and (*B*) *dcl2/4*(*FWA*^{C}) plants. Data for two independent TRV:FWAtr-infected lines per genotype are presented. Col-0(*FWA*^{Cme}) and *dcl2/4*(*FWA*^{Cme}) plants were assayed as a comparison. The position of C residues along the *FWAtr* region is represented by the ticks on the *x* axis and the context of methylation is represented by the different colors: CG is in black, CHG is in blue, and CHH is in red. The four CG residues that are demethylated in the VN by DME (24, 25) are represented by an asterisk.

Initiation and Establishment of Epigenetic Silencing. Mutation of PolV function led to complete loss of VIGS-RdDM (Fig. 3*A* and Figs. S5 and S6*A*) and it is therefore likely that this protein acts in both establishment and RNA-mediated maintenance of silencing. In other RdDM silencing systems, PolV has been implicated in the production of scaffold RNAs that are the binding site of AGO-bound sRNAs that direct DNA methylation to the adjacent chromatin (1, 2). It is anticipated that PolV has a scaffold RNA role in *FWA* promoter VIGS, as proposed for these other RdDM systems. The most abundant sRNAs in the TRV:FWAtr-infected plants are the 21/22-nt size class generated by DCL2, and DCL4 (23) (Figs. 1*A* and 3*C* and Figs. S4*A* and S7), and it is probable, as in the RDR6-RdDM system (12), that these RNAs account for the primary RdDM mediated by VIGS.

Mutation of the de novo methyltransferase DRM2 leads to complete loss of VIGS-RdDM (Fig. 3*A* and Figs. S5 and S6*A*), suggesting that DNA methylation is an early epigenetic mark in the establishment mechanism. DNA methylation at *FWAtr* could be detected in the pollen of plants undergoing VIGS-RdDM, indicating that DNA methylation is established early (Fig. 5 and Fig. S8). However, we could not detect this *FWA* promoter methylation in the vegetative tissue of Col-0(*FWA*^{C}) V_0 plants (Fig. S1*F*), and it remains possible that another process—initiation—precedes establishment of DNA methylation in the gametes. Such an alternative process could involve histone modifications (1) or it could involve persistent RNAs, like those involved in "recovery" from virus infection (26). Recovery is a long-lived and sequence-specific immunity to secondary infection by plant viruses including TRV that is mediated by RNA silencing.

Maintenance of Epigenetic Silencing. Our data indicate that, following establishment of *FWA* promoter VIGS, the epigenetic marks are maintained in the V_1 and subsequent progeny by two partially redundant maintenance mechanisms. An RNA-independent maintenance relies on the recognition of hemimethylated Cs in the symmetrical context of newly replicated DNA motifs by the DNA methyltransferases MET1 and CMT3. In contrast, the RNA-dependent maintenance is sequence motif-independent. It involves canonical PolIV-RdDM in which methyl DNA-binding proteins recruit the 24-nt sRNA biogenesis proteins to the genomic site of primary RdDM. The 24-nt sRNAs would then continue to direct the DNA methyltransferases to the unmethylated strand of newly replicated DNA. DCL3 is a key protein in this process because it generates the 24-nt sRNAs.

The *dcl3* phenotype is consistent with this interpretation because the mutation did not affect establishment but it did reduce the level of CHH methylation (Fig. 3 and Fig. S6). That there was no effect of *dcl3* on the frequency of early-flowering progeny is probably because the overall level of *FWAtr* DNA methylation in the *dcl3* mutant was similar to that observed for the wild-type, although it was more biased to CG and CHG methylation. We propose that initiation and establishment of *FWA* silencing in *dcl3* would have been as in wild-type plants but that maintenance was only via the RNA-independent mechanism.

Conclusion

Our proposed model for *FWA* promoter VIGS involves initiation and establishment mechanisms likely mediated by 21/22-nt sRNAs followed by two maintenance mechanisms that are either

PLANT BIOLOGY

dependent on 24-nt sRNAs or independent of RNA (Fig. S10). This model can account for the high level of DNA methylation at *FWAtr* in all contexts in the V_1 progeny of *dcl2/4* plants and the reduction of this strong silencing in *dcl2/3/4* V_1 progeny to levels of CG methylation that were lower than in the *dcl3* mutant (Fig. 3*B* and Fig. S6). To explain these effects, we propose that initiation and establishment of *FWA* silencing in the *dcl2/4* and *dcl2/3/4* mutants is at a lower level than in wild-type and *dcl3* because the 21/22-nt initiator sRNAs would be produced, presumably, by DCL1 alone rather than DCL1, -2, and -4 in wild-type plants. The low level of primary RdDM in the *dcl2/4* plants would be compensated for by the RNA-dependent maintenance mechanism that would be supercharged by the very abundant 24-nt sRNAs (Fig. 3*C* and Figs. S4*A* and S7).

This model could also explain the transition from PTGS to TGS of the *Evade* retroelement (27), the RDR6-RdDM pathway in which 21/22-nt sRNAs direct DNA methylation at active TEs (12), the 21-nt sRNAs from VN of pollen having a role in epigenetic modification of DNA in the SC (28), and with secondary epigenetically activated siRNAs (easiRNAs) and tasiRNAs that guide RdDM at active TEs and *TAS* genes, respectively (11, 29). The paradigm could also be reconciled with the finding that PolIV is apparently required for de novo RdDM of an *FWA* transgene in plants with an endogenous FWA^{Cme} (30). We propose that, independent of PolIV, there is very low-level silencing of this transgene similar to the establishment of silencing in our V_0 plants (Fig. 5*A*). Transgenes are often prone to spontaneous silencing because they produce aberrant RNA. However, in the presence of PolIV, 24-nt sRNAs would maintain and reinforce the silencing of this transgene. Some of these 24nt sRNAs may have been produced at FWA^{Cme} and acted *in trans* at the transgene locus.

The interpretation that 24-nt sRNAs are not sufficient for establishment is also consistent with the similar levels of 24-nt sRNAs complementary to *FWAtr* in plants with active and silent *FWA*, despite the different levels of DNA methylation at *FWAtr* (19). Similarly, in paramutation, there is evidence that 24-nt sRNAs are not sufficient to transmit silencing from one allele to another (31). It is therefore possible that the requirement for 21/22-nt sRNAs for establishment and the switch to 24-nt sRNAs for maintenance is a general feature of de novo RdDM in plants (12).

An attraction of our model is that it requires only a single process to explain diverse initiation of epigenetic silencing in many systems. However, we have not yet been able to carry out a rigorous test of the model because no mutant devoid of 21/22-nt viral sRNAs is available. In the absence of such a test we concede that a second mechanism for establishment of RdDM involving 24nt sRNAs remains possible.

In addition to mechanistic insights, our data also suggest an enhanced strategy for heritable, epigenetic VIGS of endogenous loci. The target locus should be in a *dcl2/4* mutant to establish gene silencing and there should be a functional DCL3 to ensure maximal reinforcement through the RNA-dependent maintenance mechanism. To boost the system further, a target with a high number of C residues in the CG context will ensure efficiency of the RNA-independent maintenance mechanism. This strategy may have application if epigenetic silencing would be useful for crop plant improvement.

Materials and Methods

Plant Methods. Wild-type [Col-0(FWA^{Cme})], the *fwa-d* epimutant (17) [Col-0 (FWA^{C})] and various RNA silencing mutants in the Col-0 background (Table S1) were grown using standard plant growth methods. See *SI Materials and Methods*.

Viral Inoculations. Previously described TRV VIGS vectors (15, 16) were modified to contain the *FWAtr* or *FWAcds* DNA sequences. Virus replication was carried out according to ref. 15 and young leaves of 3-wk-old *Arabidopsis* plants were mechanically inoculated. See *SI Materials and Methods*.

Nucleic Acid Analyses. Standard protocols for RNA and DNA extraction were performed. See *SI Materials and Methods* for subsequent techniques and Table S2 for oligonucleotides.

ACKNOWLEDGMENTS. We thank Sebastian Müller for bioinformatic support; Shuoya Tang and Mel Steer for technical assistance; and Ian Henderson, Tim Hore, Jake Harris, and Quentin Gouil for critical reading prior to submission. Work in the D.C.B. laboratory is supported by The Gatsby Charitable Foundation, the EU FP7 Collaborative Project Grant AENEAS, and the European Research Council Advanced Investigator Grant ERC-2013-AdG 340642. D.C.B. is the Royal Society Edward Penley Abraham Research Professor.

1. Law JA, Jacobsen SE (2010) Establishing, maintaining and modifying DNA methylation patterns in plants and animals. *Nat Rev Genet* 11(3):204–220.
2. Matzke MA, Mosher RA (2014) RNA-directed DNA methylation: An epigenetic pathway of increasing complexity. *Nat Rev Genet* 15(6):394–408.
3. Law JA, et al. (2013) Polymerase IV occupancy at RNA-directed DNA methylation sites requires SHH1. *Nature* 498(7454):385–389.
4. Zhang H, et al. (2013) DTF1 is a core component of RNA-directed DNA methylation and may assist in the recruitment of Pol IV. *Proc Natl Acad Sci USA* 110(20):8290–8295.
5. Zhong X, et al. (2014) Molecular mechanism of action of plant DRM de novo DNA methyltransferases. *Cell* 157(5):1050–1060.
6. Johnson LM, et al. (2014) SRA- and SET-domain–containing proteins link RNA polymerase V occupancy to DNA methylation. *Nature* 507(7490):124–128.
7. Liu Z-W, et al. (2014) The SET domain proteins SUVH2 and SUVH9 are required for Pol V occupancy at RNA-directed DNA methylation loci. *PLoS Genet* 10(1):e1003948.
8. Zemach A, et al. (2013) The *Arabidopsis* nucleosome remodeler DDM1 allows DNA methyltransferases to access H1-containing heterochromatin. *Cell* 153(1):193–205.
9. Stroud H, et al. (2014) Non-CG methylation patterns shape the epigenetic landscape in *Arabidopsis*. *Nat Struct Mol Biol* 21(1):64–72.
10. Pontier D, et al. (2012) NERD, a plant-specific GW protein, defines an additional RNAi-dependent chromatin-based pathway in *Arabidopsis*. *Mol Cell* 48(1):121–132.
11. Wu L, Mao L, Qi Y (2012) Roles of Dicer-like and argonaute proteins in TAS-derived small interfering RNA-triggered DNA methylation. *Plant Physiol* 160(2):990–999.
12. Nuthikattu S, et al. (2013) The initiation of epigenetic silencing of active transposable elements is triggered by RDR6 and 21-22 nucleotide small interfering RNAs. *Plant Physiol* 162(1):116–131.
13. Jones L, Ratcliff F, Baulcombe DC (2001) RNA-directed transcriptional gene silencing in plants can be inherited independently of the RNA trigger and requires Met1 for maintenance. *Curr Biol* 11(10):747–757.
14. Lu R, Martin-Hernandez AM, Peart JR, Malcuit I, Baulcombe DC (2003) Virus-induced gene silencing in plants. *Methods* 30(4):296–303.
15. Ratcliff F, Martin-Hernandez AM, Baulcombe DC (2001) Tobacco rattle virus as a vector for analysis of gene function by silencing. *Plant J* 25(2):237–245.
16. Liu Y, Schiff M, Dinesh-Kumar SP (2002) Virus-induced gene silencing in tomato. *Plant J* 31(6):777–786.
17. Kinoshita Y, et al. (2007) Control of FWA gene silencing in *Arabidopsis* thaliana by SINE-related direct repeats. *Plant J* 49(1):38–45.
18. Soppe WJJ, et al. (2000) The late flowering phenotype of *fwa* mutants is caused by gain-of-function epigenetic alleles of a homeodomain gene. *Mol Cell* 6(4):791–802.
19. Chan SW-L, Zhang X, Bernatavichute YV, Jacobsen SE (2006) Two-step recruitment of RNA-directed DNA methylation to tandem repeats. *PLoS Biol* 4(11):e363.
20. Ikeda Y, Kobayashi Y, Yamaguchi A, Abe M, Araki T (2007) Molecular basis of late-flowering phenotype caused by dominant epi-alleles of the FWA locus in *Arabidopsis*. *Plant Cell Physiol* 48(2):205–220.
21. Bologna NG, Voinnet O (2014) The diversity, biogenesis, and activities of endogenous silencing small RNAs in *Arabidopsis*. *Annu Rev Plant Biol* 65:473–503.
22. Henderson IR, et al. (2006) Dissecting *Arabidopsis thaliana* DICER function in small RNA processing, gene silencing and DNA methylation patterning. *Nat Genet* 38(6):721–725.
23. Deleris A, et al. (2006) Hierarchical action and inhibition of plant Dicer-like proteins in antiviral defense. *Science* 313(5783):68–71.
24. Schoft VK, et al. (2011) Function of the DEMETER DNA glycosylase in the *Arabidopsis thaliana* male gametophyte. *Proc Natl Acad Sci USA* 108(19):8042–8047.
25. Calarco JP, et al. (2012) Reprogramming of DNA methylation in pollen guides epigenetic inheritance via small RNA. *Cell* 151(1):194–205.
26. MacDiarmid R (2005) RNA silencing in productive virus infections. *Annu Rev Phytopathol* 43:523–544.
27. Marí-Ordóñez A, et al. (2013) Reconstructing de novo silencing of an active plant retrotransposon. *Nat Genet* 45(9):1029–1039.
28. Slotkin RK, et al. (2009) Epigenetic reprogramming and small RNA silencing of transposable elements in pollen. *Cell* 136(3):461–472.
29. Creasey KM, et al. (2014) miRNAs trigger widespread epigenetically activated siRNAs from transposons in *Arabidopsis*. *Nature* 508(7496):411–415.
30. Chan SW-L, et al. (2004) RNA silencing genes control de novo DNA methylation. *Science* 303(5662):1336.
31. Hollick JB (2012) Paramutation: A *trans*-homolog interaction affecting heritable gene regulation. *Curr Opin Plant Biol* 15(5):536–543.

Supporting Information

Supporting Information Corrected March 30, 2015

Bond and Baulcombe 10.1073/pnas.1413053112

SI Materials and Methods

Plant Methods. Wild-type [Col-0(FWA^{Cme})], the *fwa-d* epimutant (1) [Col-0(FWA^{C})] and various RNA silencing mutants of *Arabidopsis thaliana* in the Col-0 background (Table S1), but introgressed into the *fwa-d* epimutant, were grown on soil (Levington F2):vermiculate (fine) mix (ratio of 5:1) in a Conviron controlled environment growth room at 20 °C with 16-h light and 8-h dark periods, 60% relative humidity, and 150 μmol·m^2·s light intensity. Wild-type [Ler(FWA^{Cme})] and the *fwa-2* epimutant (2) [Ler(FWA^{C})] (obtained from Nottingham Arabidopsis Stock Centre) were also used in this study.

Flowering time was measured by counting the total number of rosette leaves at the time of bolting. Plants with ≤16 leaves were considered to be early flowering; plants with 17–22 leaves were considered to be intermediate flowering; plants with ≥23 leaves were considered to be late flowering. Unless otherwise stated in the figure legends, the total rosette leaf number was measured from ∼48 individual plants from each line presented.

Viral Inoculations. The construction of two sets of infectious binary vectors containing RNA1 and RNA2 of the bipartite RNA virus Tobacco Rattle Virus (TRV) have been previously described (3, 4). TRV:FWAtr and TRV:FWAcds were constructed by ligating the *FWAtr* and *FWAcds* (Fig. S1*A*) fragments with the BamHI or BamHI/XhoI sites within the multiple cloning sites of the different RNA2 binary vectors. TRV:FWAtr carries a 544-bp fragment, corresponding to the "B region" that is required for *FWA* silencing by an inverted repeat (1). TRV:FWAcds carries a 475-bp fragment corresponding to Exon 3 of *FWA*.

To generate a TRV infection, the RNA1, RNA2, and modified RNA2 binary vectors were transformed into *Agrobacterium tumefaciens* (strain GV3101:pMP90 + pSOUP) and coinfiltrated into young leaves of wild-type *Nicotiana benthamina* plants to increase virus replication, as described previously (3). To infect *Arabidopsis thaliana*, young leaves of infiltrated *N. benthamiana* plants were harvested 7 dpi and ground in 10 mM sodium phosphate buffer (pH 7.0). Young leaves of 3-wk-old *Arabidopsis* plants were dusted with carborundum and 10 μL of viral extract from *N. benthamiana* was used for mechanical inoculation. Tissue samples for RNA analysis where harvested 14 dpi (rosette leaves) to determine the level of viral infection. Further tissue samples were collected for RNA and DNA analysis at different time points as described in the figure legends.

DNA Analyses. DNA samples were prepared from ∼50 mg of leaf tissue or mixed inflorescence tissue using Qiagen Puregene reagents (5).

DNA from pollen was extracted using modified protocols previously described (6, 7). Briefly, open flowers were harvested into a 2-mL Eppendorf tube on ice containing 1.5 mL Galbraith Buffer (8). Tubes were vortexed vigorsly for 3 min to release mature pollen grains. The crude fraction was filtered through a 40-μm filter into a 50-mL falcon tube, on ice. The Eppendorf tube and filter were washed with 5 mL Galbraith Buffer, and the wash was passed through the again filter to include as many pollen grains as possible. The pollen suspension was spun at 150 × *g* for 10 min at +4 °C. The supernatant was removed and the pellet of pollen cells was resuspended in 400 μL pollen lysis buffer (100 mM NaCl, 50 mM Tris·HCl pH 8.0, 1 mM EDTA, 1% SDS, 1 mM DTT) and added to a clean 1.5-mL Eppendorf tube. Proteinase K (20 μg/mL) was added and the samples were incubated at 65 °C for 4 h with occasional homogenization. Approximately, 100 μL of acid-wash 1-mm glass beads (Sigma) were added and the tubes were vortexed vigorsly for 3–4 min to disrupt the pollen grains. DNA was purified using phenol:chloroform:isoamyl alcohol solution (Sigma) and standard ethanol precipitation followed by resuspension in 1× TE.

To test for the level of DNA methylation we performed McrBC-qPCR. For McrBC assays, 100 ng of DNA was added to the following components: 1× NEB Buffer 2, 10 μg BSA, 1 mM GTP in a final volume of 100 μL. The reaction was split into two; 50 ng of DNA was digested at 37 °C for 6 h with 10 U of McrBC (New England Biolabs) or 50 ng was treated with mock digestion conditions [1 μL of 50% (vol/vol) glycerol]. The reactions were inactivated at 65 °C, 20 min. For quantitative PCR (qPCR), 2 ng of DNA (± McrBC) was added to 18 μL of the following reaction mix: 1× Roche buffer (10 mM Tris·HCl, 50 mM KCl, pH 8.3), 4 mM $MgCl_2$, 0.2 mM dNTPs, 0.15 μM of each primer, 0.5× SYBR Green I (Life Technologies), and 0.25 U of GoTaq DNA polymerase (Promega). Standard qPCR cycling conditions were used (annealing temperature of 58 °C) and at least two technical replicates were performed for all samples. See Table S2 for list of oligonucleotides used for McrBC-qPCR. Results are expressed as a percentage of methylation, or loss of DNA molecules (reduced amplification) as a result of McrBC digestion $[(\{1/2^{-Ct\ digested}\}/\{1/2^{-Ct\ undigested}\}) \times 100]$.

To determine the context of DNA methylation, bisulfite sequencing was performed. For analysis of DNA from leaf tissue, 500 ng of DNA was converted using EZ DNA Methylation-Gold Kit (Zymo Research). Approximately 50 ng of bisulfite-treated DNA was used in the following PCR mix: GoTaq buffer, 2 mM $MgCl_2$, 0.2 mM dNTPs, 5% (vol/vol) DMSO, 0.4 mM of each primer, and 2.5 units of GoTaq DNA polymerase (Promega). Nested PCR was performed for bisulfite sequencing of *FWA*; 1 μL of the first-round PCR was used as template for the second round of PCR with the same reaction conditions. See Table S2 for list of oligonucleotides used for bisulfite sequencing. Approximately 16 clones were sequenced. Bisulfite-converted sequences were aligned to the *FWAtr* DNA sequence using ClustalX. Evaluation of percentage methylation and context of methylation was performed using CyMate (9).

For bisulfite sequencing analysis of DNA from pollen, 50 ng of DNA was converted using EZ DNA Methylation-Gold Kit (Zymo Research). Approximately 20 ng of bisulfite-treated DNA was used in a PCR using KAPA HiFi HotStart Uracil+ ReadyMix (KAPA Biosystems) following the manufacturer's instructions. The primers used for bisulfite sequencing of pollen DNA were modified versions of the primers used for the nested PCR for bisulfite sequencing of leaf DNA (Table S2). For each sample, 40–48 clones were sequenced and analyzed as described above.

RNA Analyses. Total RNA samples were prepared from 100 mg of leaf tissue or mixed inflorescence tissue using TRIzol (Life Technologies).

For cDNA synthesis, 5 μg of total RNA was first DNase treated using Turbo DNase (Ambion), following the manufacturer's guidelines. cDNA was then synthesized using random hexamers and SuperScript III (Life Technologies), according to the protocol. For qPCR, cDNA samples were diluted 10-fold and 5 μL was used in a 20-μL final qPCR reaction, as described above for McrBC assays. Three technical replicates were performed for each gene per sample analyzed. Comparative quantification analysis was used to determine the relative expression of the gene of interest compared with a control gene (*FDH – At5g43940*) in each sample

(10). For RT-PCR, 5 μL of diluted (10-fold) cDNA was added to 15 μL of the following reaction mix: 1× GoTaq buffer, 4 mM $MgCl_2$, 0.2 mM dNTPs, 0.15 μM of each primer, and 0.25 U of GoTaq DNA polymerase (Promega). See Table S2 for list of oligonucleotides used for qPCR and RT-PCR.

For Northern blots, total RNA (10 μg) was dried down and resuspended in 5 μL loading buffer [0.10% Bromophenol Blue and 0.10% Xylene Cyanol in 100% (vol/vol) de-ionized Formamide], heated at 95 °C for 3 min, and loaded onto a 1× Mops/1% Formaldehyde/1.5% (wt/vol) agarose gel (for high molecular weight RNA) or onto a 15% (wt/vol) PAGE/7 M Urea gel. Following electrophoresis, RNA was transferred to HyBond N+ (GE Healthcare) using capillary transfer. PCR products (see Table S2 for oligonucleotides used for PCR amplifications) were radioactively labeled with ^{32}P using Rediprime II (Amersham) or Oligonucleotide probes (Table S2) were end-labeled with ^{32}P by Polynucleotide Kinase (New England Biolabs). All probes were purified through a MicroSpin G-25 column (GE Healthcare) according to the manufacturers' recommendations. Long RNA Northern hybridizations were performed at 65 °C with PerfectHyb Plus (Sigma) and small RNA Northern hybridizations at 42 °C with PerfectHyb Plus for long probes or 37 °C with UltraHyb-Oligo buffer (Ambion) for oligo probes. Radioactive signals were detected after exposure of the membrane to a phosphor image screen using a Typhoon Molecular Imager (GE Healthcare).

To test for the presence of TRV:FWAtr in the progeny of infected plants, OneStep qPCR was performed using Precision OneStep qRT-PCR Mastermix (Primerdesign). For each plant, total RNA was extracted (as described above) and diluted to a working concentration of 10 ng/μL. For each PCR, 50 ng of RNA was added according to the manufacturer's instructions. The level of *FDH* expression was used as a positive control for each RNA sample. See Table S2 for list of oligonucleotides used for OneStep PCR.

Small RNA Cloning. To clone sRNAs, 10 μg of total RNA was run on a 15% (wt/vol) PAGE/7 M Urea gel, and following electrophoresis the sRNA fraction (18–32 nt) was excised and eluted from the gel. To avoid contamination, RNA samples from mock-infected plants (1× for wild-type and 1× for the *dcl2/4* mutant) were run on different gels than the RNA from TRV:FWAtr-infected plants (3× for each genotype). sRNAs were subsequently cloned using the Illumina TruSeq Small RNA cloning kit and libraries were indexed during the PCR step (12 cycles) according to the manufacturer's protocol. The same amount of each sRNA library was pooled and run on a NextSeq. 500 (Illumina). The sRNA sequencing data are available in the ArrayExpress database under accession no. E-MTAB-3009.

Bioinformatic Analyses. sRNA reads were trimmed using Trimmomatic (11) and mapped to the *FWAtr* target sequence (Chr4: 13038238–13038777) using Bowtie 1.1.1 (12). The distribution of all reads mapping to *FWAtr* were plotted using a custom R script (courtesy of Sebastian Müller, Department of Plant Sciences, University of Cambridge, Cambridge, UK) and ggplot2 (13). The proportion of 21-nt, 22-nt, 23-nt, and 24-nt sRNA reads mapping to *FWAtr* was determined from the actual read count, corrected for multiple mapping, and normalized to the size of the sRNA library.

1. Kinoshita Y, et al. (2007) Control of FWA gene silencing in *Arabidopsis thaliana* by SINE-related direct repeats. *Plant J* 49(1):38–45.
2. Soppe WJJ, et al. (2000) The late flowering phenotype of fwa mutants is caused by gain-of-function epigenetic alleles of a homeodomain gene. *Mol Cell* 6(4):791–802.
3. Ratcliff F, Martin-Hernandez AM, Baulcombe DC (2001) Technical advance. Tobacco rattle virus as a vector for analysis of gene function by silencing. *Plant J* 25(2):237–245.
4. Liu Y, Schiff M, Dinesh-Kumar SP (2002) Virus-induced gene silencing in tomato. *Plant J* 31(6):777–786.
5. Havecker ER, Wallbridge LM, Fedito P, Hardcastle TJ, Baulcombe DC (2012) Metastable differentially methylated regions within *Arabidopsis* inbred populations are associated with modified expression of non-coding transcripts. *PLoS ONE* 7(9):e45242.
6. Calarco JP, et al. (2012) Reprogramming of DNA methylation in pollen guides epigenetic inheritance via small RNA. *Cell* 151(1):194–205.
7. Drouaud J, Mézard C (2011) DNA recombination: Characterization of meiotic crossovers in pollen from *Arabidopsis thaliana*. *Methods in Molecular Biology*, ed Tsubouchi H (Humana, Totowa, NJ), pp 223–249.
8. Galbraith DW, et al. (1983) Rapid flow cytometric analysis of the cell cycle in intact plant tissues. *Science* 220(4601):1049–1051.
9. Hetzl J, Foerster AM, Raidl G, Mittelsten Scheid O (2007) CyMATE: A new tool for methylation analysis of plant genomic DNA after bisulphite sequencing. *Plant J* 51(3):526–536.
10. Bond DM, Dennis ES, Pogson BJ, Finnegan EJ (2009) Histone acetylation, VERNALIZATION INSENSITIVE 3, FLOWERING LOCUS C, and the vernalization response. *Mol Plant* 2(4):724–737.
11. Bolger AM, Lohse M, Usadel B (2014) Trimmomatic: A flexible trimmer for Illumina sequence data. *Bioinformatics* 30(15):2114–2120.
12. Langmead B, Trapnell C, Pop M, Salzberg SL (2009) Ultrafast and memory-efficient alignment of short DNA sequences to the human genome. *Genome Biol* 10(3):R25.
13. Wickham H (2009) *ggplot2: Elegant Graphics for Data Analysis.* (Springer, New York).

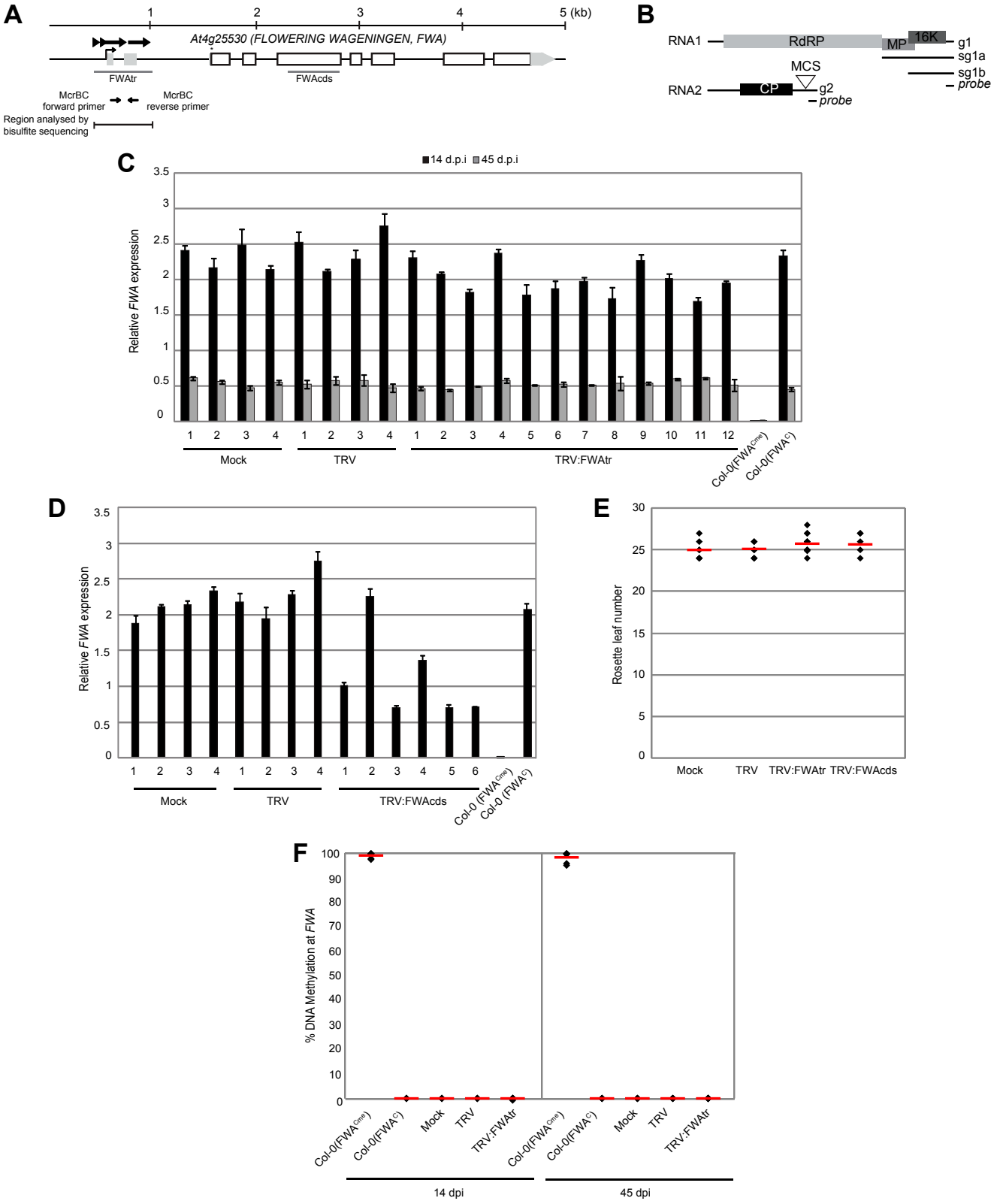

Fig. S1. VIGS of *FWA* in infected *Arabidopsis* plants. (*A*) Gene structure of *FWA* (At4g25530). The position of the tandem repeats in the promoter and 5′UTR region of *FWA* are drawn as bold black arrows. The regions of the tandem repeat and coding sequence that were cloned into TRV, to make TRV:FWAtr and TRV:FWAcds, respectively, are highlighted in dark gray. The position of primers used for McrBC-qPCR and the region analyzed by bisulfite sequencing are highlighted. Coding exons are drawn as white boxes and UTR exons as gray boxes. Start of transcription is represented by an upward arrow and start of translation is represented by an asrterisk. (*B*) Schematic diagram of the TRV bipartite genome (comprised of RNA1 and RNA2) with the position of the probe used to detect all TRV viral RNA species via Northern blot. The multiple cloning site (MCS) within RNA2 is used for inserting the DNA sequence of interest. Data

Legend continued on following page

from ref. 3. RdRP: RNA-dependent RNA Polymerase; MP: Movement protein; 16K: 16kD protein; CP: Coat protein; g1: genomic 1; g2: genomic 2; sg1a: subgenomic 1a; sg1b: subgenomic 1b. Refer to ref. 3 for more information. (*C*) *FWA* expression (relative to *FDH*) in Col-0(FWA^{C}) plants infected with TRV:FWAtr, TRV, or mock conditions. RNA was sampled from leaf tissue 14 dpi (black bars) and floral tissue 45 dpi (gray bars). RNA from Col-0(FWA^{Cme}) and Col-0 (FWA^{C}) plants of the same age was included as a comparison, except floral tissue from Col-0(FWA^{Cme}) was sampled 30 dpi because these plants flowered earlier than Col-0(FWA^{C}) plants. Error bars represent the SD of the mean of technical replicates. See Fig. 1*A* for Northern blot analysis of viral RNA in these samples. (*D*) *FWA* expression (relative to *FDH*) in Col-0(FWA^{C}) plants infected with TRV:FWAcds, TRV, or mock conditions, 14 dpi. RNA from Col-0(FWA^{Cme}) and Col-0(FWA^{C}) leaf tissue of the same age was included as a comparison. Error bars represent the SD of the mean of technical replicates. See Fig. 1*A* for RT-PCR analysis of viral RNA in these samples. (*E*) Flowering time (average rosette leaf number) of Col-0(FWA^{C}) plants infected with mock, TRV, TRV:FWAtr, or TRV:FWAcds conditions (from Fig. 1 *A* and *B*). Each plant is represented by a black diamond and the average of all samples per treatment is represented by the red horizontal line. (*F*) The level of DNA methylation (McrBC-qPCR) at *FWA* in Col-0(FWA^{C}) plants infected with TRV:FWAtr, TRV, or mock conditions. DNA was sampled from leaf tissue, 14 dpi, and floral tissue, 45 dpi. DNA from Col-0 (FWA^{Cme}) and Col-0 (FWA^{C}) plants of the same age was included as a comparison, except floral tissue from Col-0 (FWA^{Cme}) was sampled 30 dpi as these plants flowered earlier than Col-0 (FWA^{C}) plants. Each sample is represented by a black diamond and the average of all samples per treatment is represented by the red horizontal line. See Fig. 1*A* for Northern blot analysis of viral RNA in these samples.

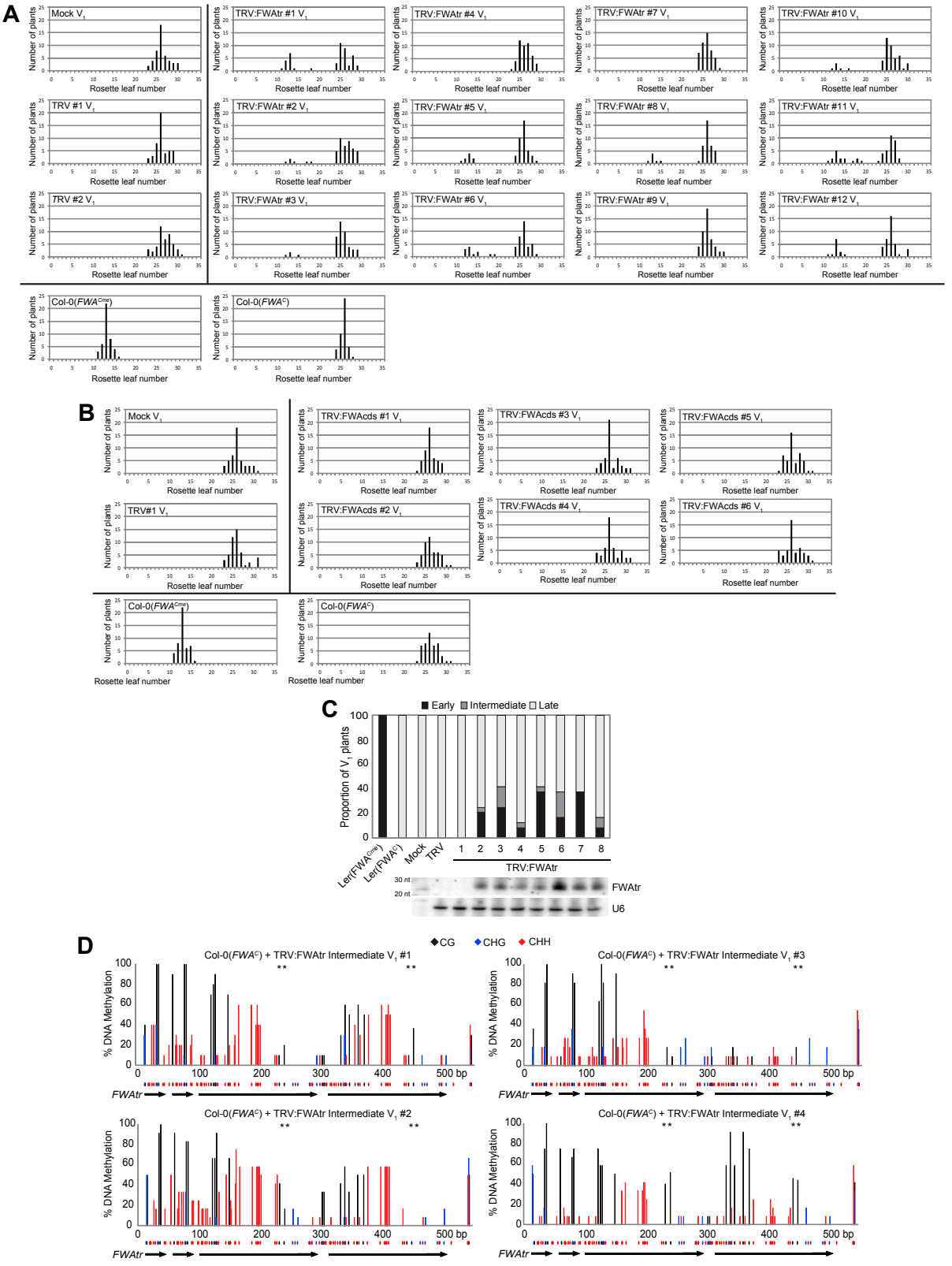

Fig. S2. Progeny of TRV:FWAtr-infected plants have a flowering-time behavior that correlates with the level of DNA methylation at *FWA*. (*A*) Flowering time (rosette leaf number) of the V_1 progeny of TRV:FWAtr-, TRV-, or mock-infected plants. Approximately 48 individual plants from each line assayed for viral infection in Fig. 1*A* were analyzed. Col-0(FWA^{Cme}) and Col-0(FWA^{C}) plants were grown at the same time as a comparison. (*B*) Flowering time (rosette leaf number) of the V_1 progeny of TRV:FWAcds-, TRV-, or mock-infected plants. Approximately 48 individual plants, from each line assayed for viral infection in Fig. 1*B*, were analyzed. Col-0(FWA^{Cme}) and Col-0(FWA^{C}) plants were grown at the same time as a comparison. (*C*, *Upper*) Proportion of early- (black), intermediate- (dark gray), and late- (light gray) flowering V_1 progeny plants from TRV:FWAtr-, TRV-, or mock-infected Ler(FWA^{C}) plants. Ler(FWA^{Cme}) and

Legend continued on following page

Ler(*FWA*^{C}) plants were grown and measured at the same time. The total rosette leaf number was measured from ~48 individual plants from each line assayed in the lower section. (*Lower*) sRNA Northern blot analysis of *FWAtr* sRNAs from leaves of TRV:FWAtr-, TRV-, or mock-infected Ler(*FWA*^{C}) plants, 14 dpi. *U6* was probed as a loading control. (*D*) Bisulfite sequencing analysis of DNA methylation at *FWAtr* in representative intermediate-flowering V_1 progeny of TRV:FWAtr-infected Col-0(*FWA*^{C}) plants. The level of DNA methylation, as determined by McrBC qPCR (Fig. 2*A*), was less than 80%. Bisulfite sequencing analysis of DNA from early-flowering siblings, and Col-0(*FWA*^{Cme}) and Col-0(*FWA*^{C}) plants of the same age are given in Fig. 2*B*. The position of C residues along the *FWAtr* region is represented by the ticks on the *x* axis and the context of methylation is represented by the different colors: CG is in black, CHG is in blue, and CHH is in red. The four CG residues that are actively demethylated in the vegetative nucleus (VN) by DME (1, 2) are represented by an asterisk.

1. Calarco JP, et al. (2012) Reprogramming of DNA methylation in pollen guides epigenetic inheritance via small RNA. *Cell* 151(1):194–205.
2. Schoft VK, et al. (2011) Function of the DEMETER DNA glycosylase in the *Arabidopsis thaliana* male gametophyte. *Proc Natl Acad Sci USA* 108(19):8042–8047.

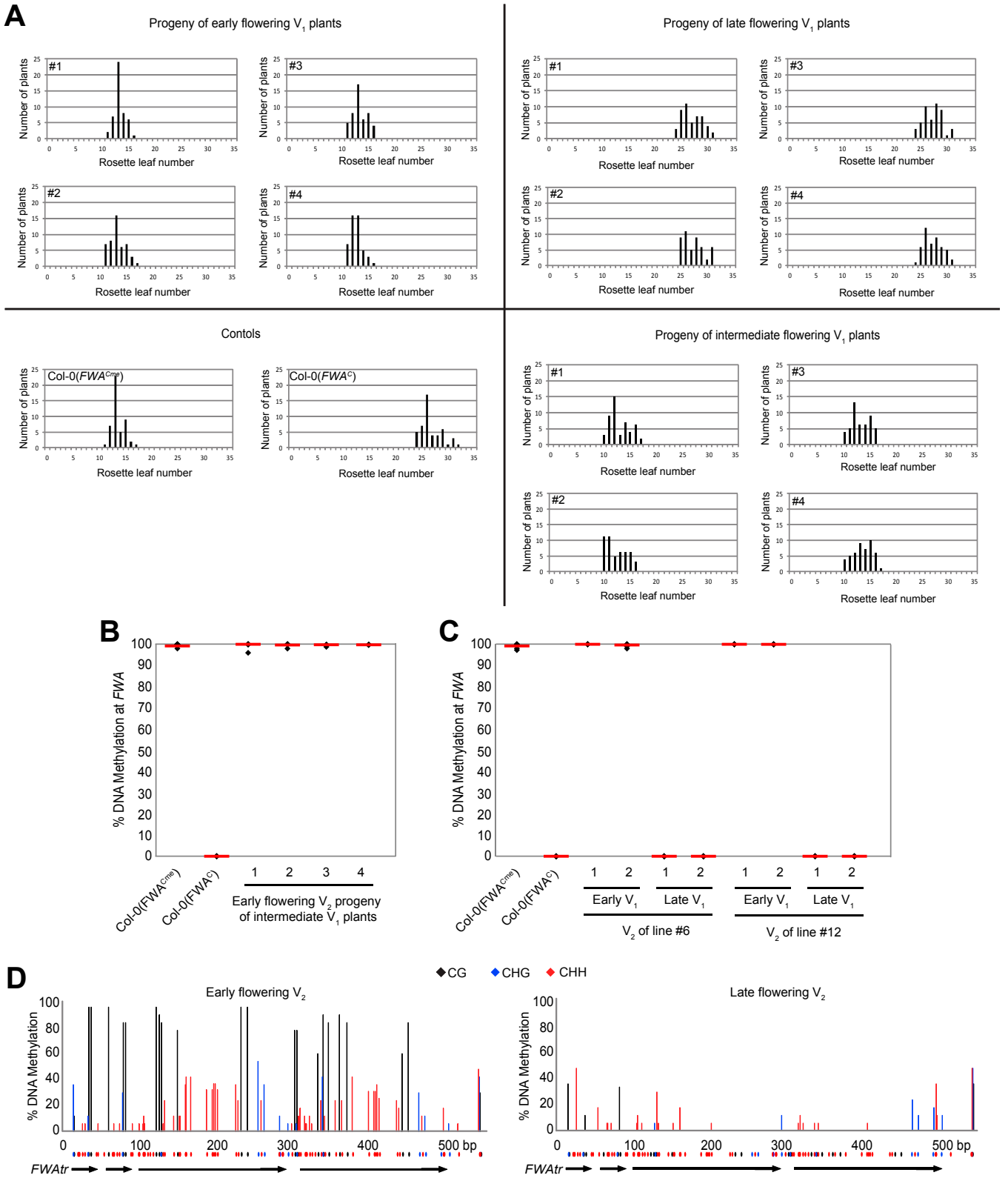

Fig. S3. VIGS of *FWA* with TRV:FWAtr establishes heritable, stable silencing. (*A*) Flowering time (rosette leaf number) of the V_2 progeny of early-, intermediate-, and late-flowering V_1 plants. Approximately 48 individual progeny plants from representative V_1 plants that showed 100% (early flowering), less than 100% (intermediate flowering), or 0% (late flowering) methylation (Fig. 2*A*) were assayed. Col-0(FWA^{Cme}) and Col-0(FWA^{C}) plants were grown at the same time as a comparison. (*B*) The level of DNA methylation at *FWA* (McrBC-qPCR) in V_2 progeny of intermediate-flowering V_1 plants. Leaf tissue was taken from six representative early-flowering V_2 plants from the progeny of four intermediate-flowering V_1 lines (*A*). Each sample is represented by a black diamond and the average of all samples per treatment is represented by the red horizontal line. (*C*) The level of DNA methylation at *FWA* (McrBC-qPCR) in V_2 progeny of

Legend continued on following page

early- and late-flowering V_1 plants (from lines 6 and 12 in Figs. 1*A* and 2*A*). Leaf tissue was taken from six representative plants that respectively maintained an early-flowering and late-flowering phenotype (*A*). Each sample is represented by a black diamond and the average of all samples per treatment is represented by the red horizontal line. (*D*) Bisulfite sequencing analysis of DNA methylation at *FWAtr* in a representative early- and late-flowering V_2 plant that maintained the flowering time phenotype of their parent plant. The position of C residues along the *FWAtr* region is represented by the ticks on the *x* axis and the context of methylation is represented by the different colors: CG is in black, CHG is in blue, and CHH is in red.

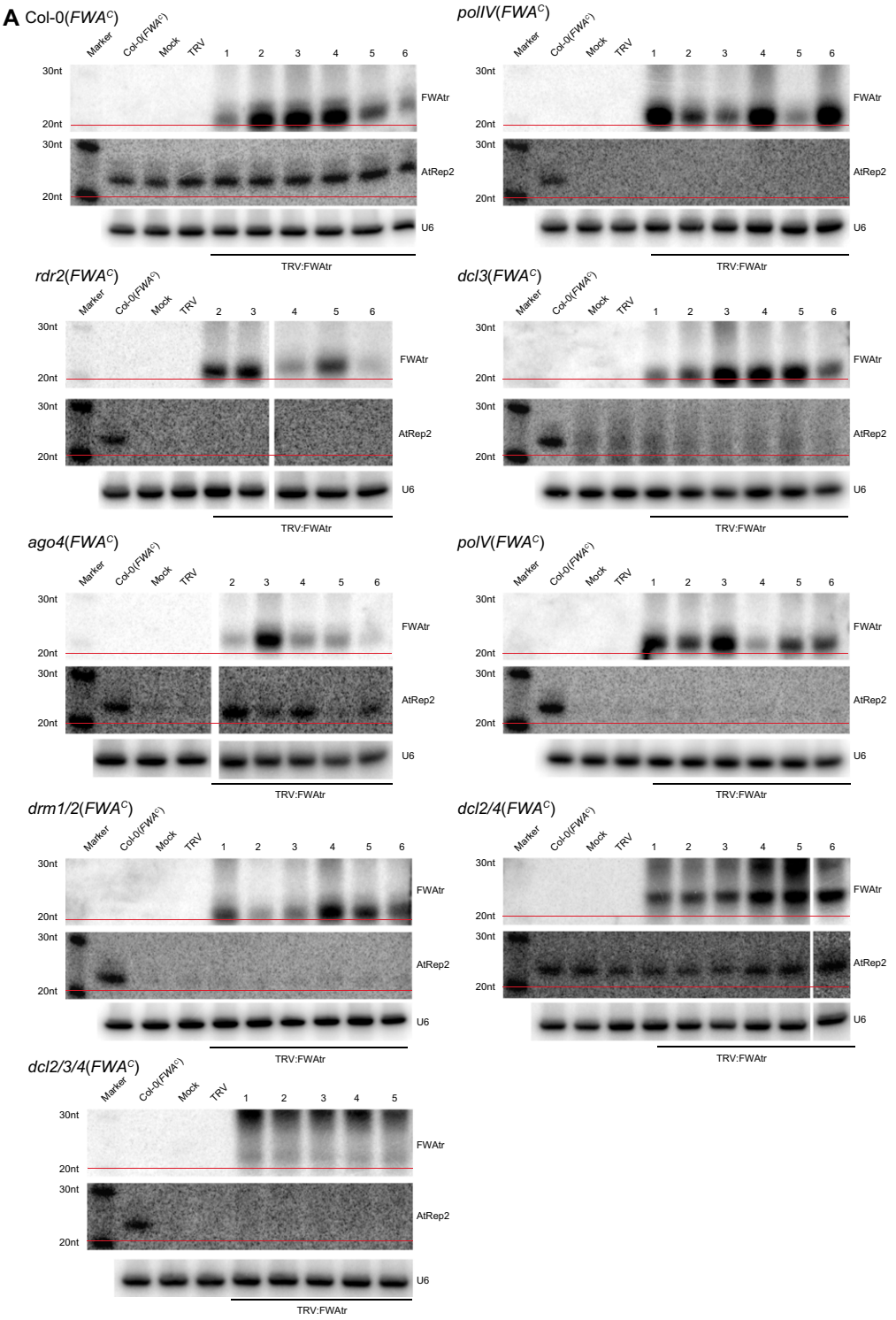

Fig. S4. (Continued)

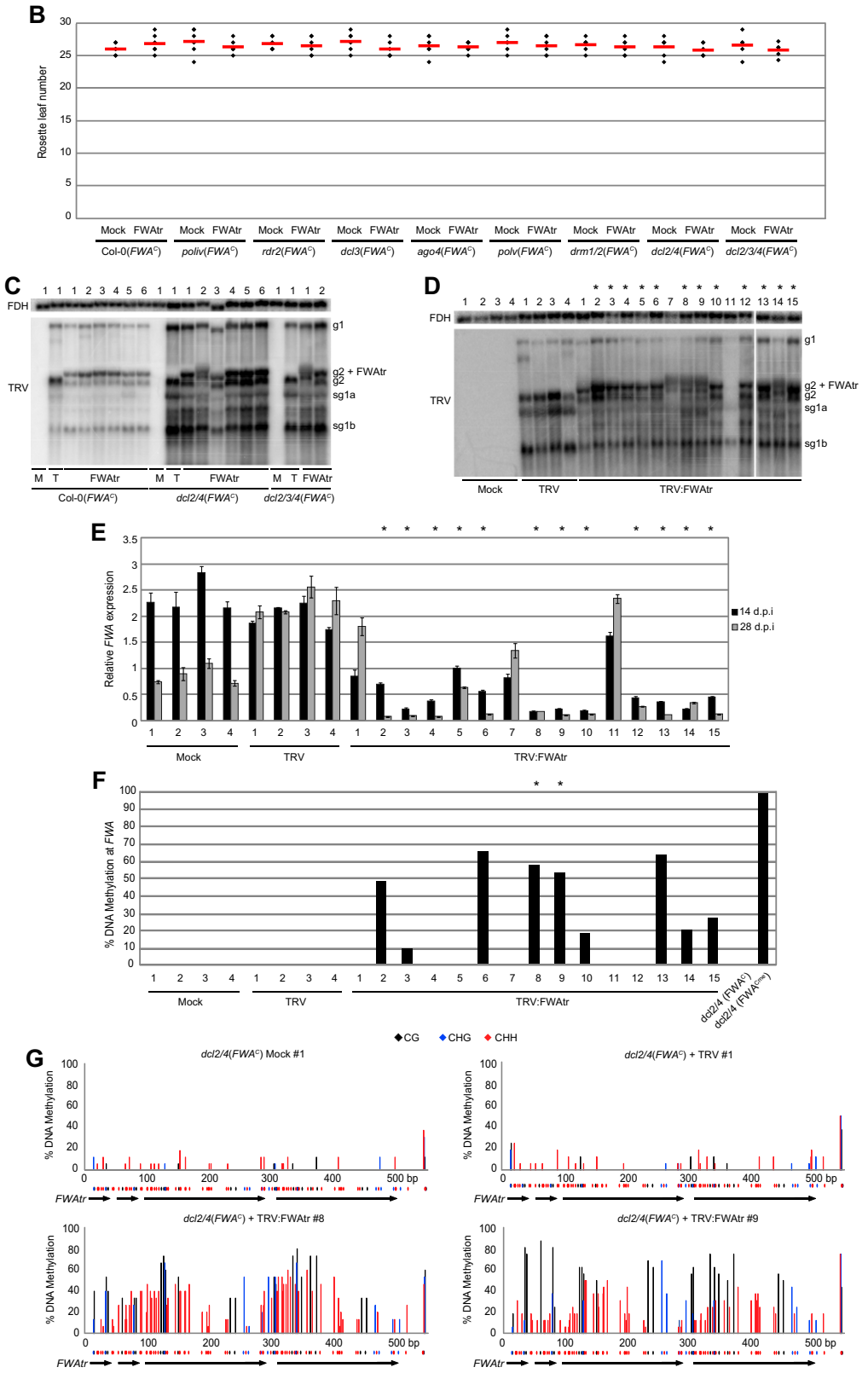

Fig. S4. Analysis of viral infection in RNA silencing mutants and their effect on VIGS-RdDM. (*A*) sRNA Northern blot analysis of *FWAtr* sRNAs from leaves of Col-0(FWA^C), *poliv*(FWA^C), *rdr2*(FWA^C), *dcl3*(FWA^C), *ago4*(FWA^C), *polv*(FWA^C), *drm1/2*(FWA^C), *dcl2/4*(FWA^C), and *dcl2/3/4*(FWA^C) plants infected with TRV:FWAtr, TRV, or mock conditions. sRNA Northern blots were also probed with *AtRep2*, a helitron-like DNA transposon with dispersed repeats in the *Arabidopsis* genome that is regulated by PolIV-RdDM, to show the effect of the different RNA silencing mutants on the production of 24-nt sRNAs. U6 was probed as an internal, loading control. For the sRNA Northern blot analysis of *rdr2*(FWA^C), the blot was cut to remove samples not used in further analyses; the area cut is

Legend continued on following page

indicated by the white separating line between lane 6 and 8 (removing lane 7). For the sRNA Northern blot analysis of *ago4*(*FWA*^{C}), the blot was cut to remove samples not used in further analyses; the area cut is indicated by the white separating line between lane 4 and 6 (removing lane 5). For the sRNA Northern blot analysis of *dcl2/4*(FWAC), TRV:FWAtr-infected samples 1–5 were run on a separate gel as indicated by the white separating line between samples 5 and 6. The position of the 20-nt marker is represented as a red line across each blot to help distinguish the size class of *FWAtr* and *AtRep2* sRNAs. (*B*) Flowering time (average rosette leaf number) of plants infected with mock or TRV:FWAtr conditions from *A*. Each plant is represented by a black diamond and the average flowering time of all plants per genotype/treatment is represented by the red horizontal line. (*C*) Northern blot analysis comparing TRV RNA species in Col-0(*FWAC*), dcl2/4(*FWAC*), and dcl2/3/4(*FWAC*) plants infected with TRV:FWAtr (FWAtr), TRV (T), or mock (M) conditions. The position of the probe used to detect the TRV RNA species is given in Fig. S1*B*. *FDH* was probed as an internal loading control. The RNA samples probed in this figure are also presented in the sRNA Northern blots presented in *A*. (*D*) Northern blot analysis of TRV RNA species in *dcl2/4*(*FWAC*) plants infected with TRV:FWAtr, TRV, or mock conditions. The position of the probe used to detect the TRV RNA species is given in Fig. S1*B*. *FDH* was probed as an internal loading control. The RNA samples probed on this Northern blot are from an independent experiment from the data presented in *A* and *C* for this genotype. Lines with a high level of infection that result in repression of *FWA* (*E*) are marked with an asterisk. TRV:FWAtr-infected samples 13–15 were run on a separate gel as indicated by the white separating line between samples 12 and 13. (*E*) *FWA* expression (relative to *FDH*) in *dcl2/4*(*FWAC*) plants infected with TRV:FWAtr, TRV, or mock conditions. RNA was sampled from leaf tissue, 14 dpi (black bars) and 28 dpi (gray bars). Error bars represent the SD of the mean of technical replicates. See *D* for level of virus infection. Lines with high viral load and repression of *FWA* that is maintained 28 dpi are marked with an asterisk. A two-tailed Student *t* test suggested *FWA* expression was repressed by infection with TRV:FWAtr (**$P < 0.01$) 14 dpi, but not with TRV (compared with infection with the mock treatment). Expression of *FWA* is repressed upon flowering; mock-infected (but not TRV- or TRV:FWAtr-infected) *dcl2/4*(*FWAC*) plants were flowering when 28-dpi samples were harvested [this difference was not observed with Col-0(*FWAC*) plants]. There was no change in the number of rosette leaves at the time of flowering (see *B*). Therefore, a two-tailed Student *t* test suggested *FWA* expression was repressed by infection with TRV:FWAtr (**P <0.01) 28 dpi, compared with infection with TRV (but not mock-infected conditions). (*F*) The level of DNA methylation at *FWA* (McrBC-qPCR) in *dcl2/4*(*FWAC*) plants infected with TRV:FWAtr, TRV, or mock conditions. DNA was sampled from floral tissue (mock-infected plants) or leaf tissue (TRV- and TRV:FWAtr-infected plants), 39 dpi. DNA from *dcl2/4*(*FWACme*) and *dcl2/4*(*FWAC*) plants was included as a comparison. Refer to *D* for Northern blot analysis of viral RNA in these plants and *E* for *FWA* expression in these lines. (*G*) Bisulfite sequencing analysis of DNA methylation at *FWAtr* in mock-, TRV-, and TRV:FWAtr-infected *dcl2/4*(*FWAC*) plants. DNA samples included in this analysis are from *E* and marked with an asterisk (lines 8 and 9). See *D* and *E* for analysis of RNA from these lines. The position of C residues along the *FWAtr* region is represented by the ticks on the *x* axis and the context of methylation is represented by the different colors: CG is in black, CHG is in blue, and CHH is in red.

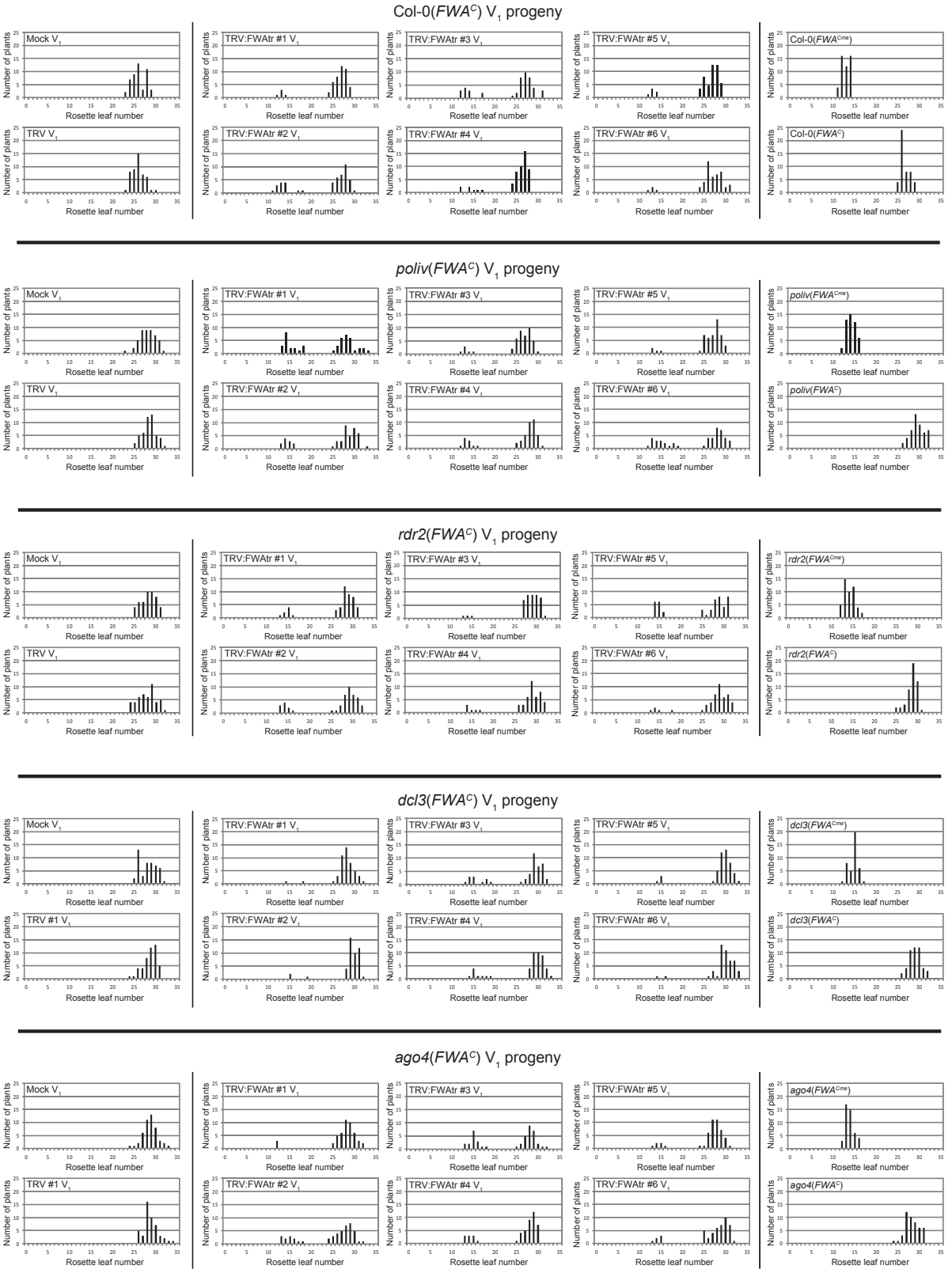

Fig. S5. (Continued)

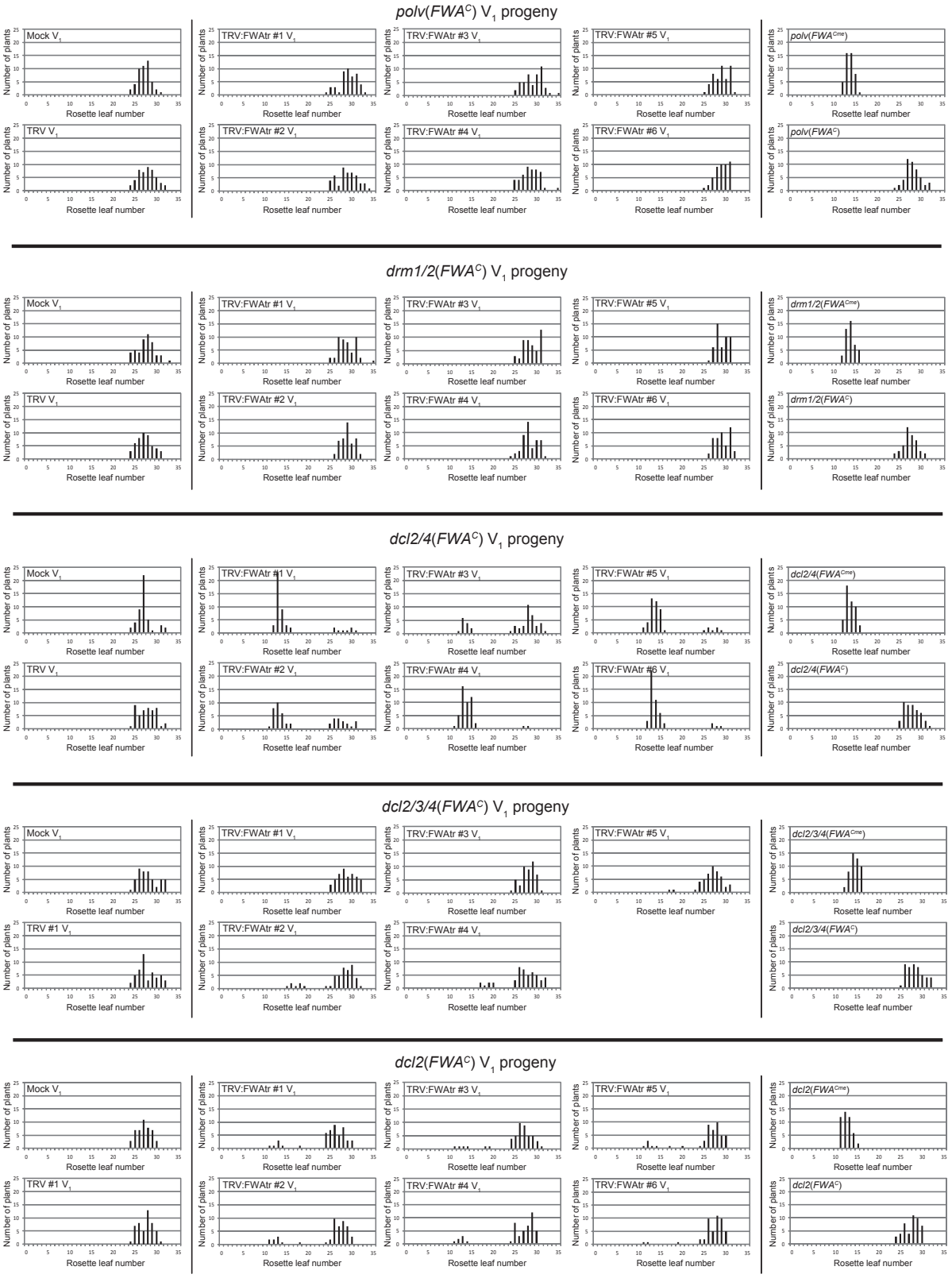

Fig. S5. (Continued)

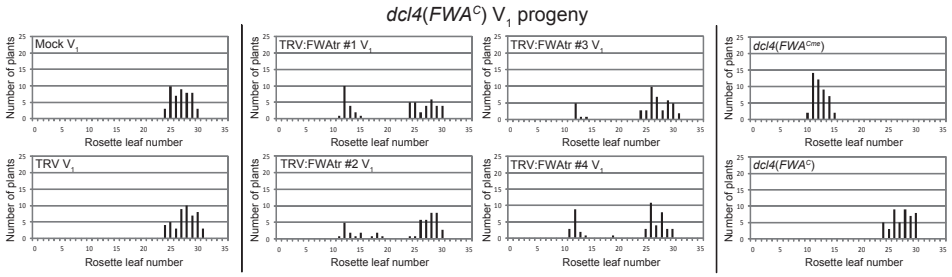

Fig. S5. VIGS-RdDM of *FWA* requires PolV and DRM1/2. Flowering time (rosette leaf number) of the V_1 progeny of Col-0(*FWA*^{C}), *polIV*(*FWA*^{C}), *rdr2*(*FWA*^{C}), *dcl3*(*FWA*^{C}), *ago4*(*FWA*^{C}), *polV*(*FWA*^{C}), *drm1/2*(*FWA*^{C}), *dcl2/4*(*FWA*^{C}), *dcl2/3/4*(*FWA*^{C}), *dcl2*(*FWA*^{C}), and *dcl4*(*FWA*^{C}) plants infected with TRV:FWAtr, TRV, or mock conditions. Approximately 48 individual progeny plants from each line assayed for viral infection (Fig. S4*A*) were analyzed. Wild-type and mutant plants (with an active or silent *FWA*) were grown at the same time as a comparison for each genotype.

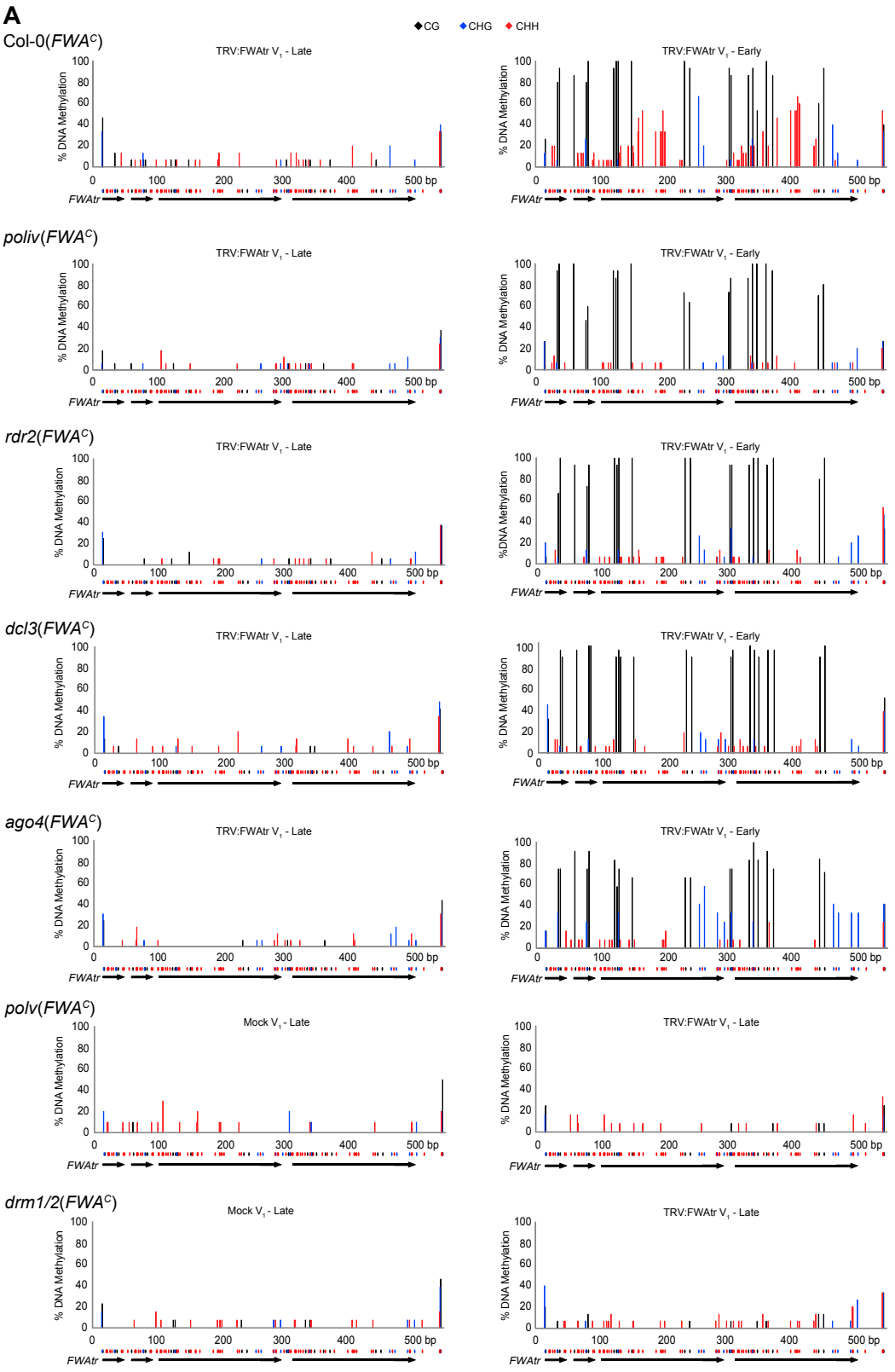

Fig. S6. (Continued)

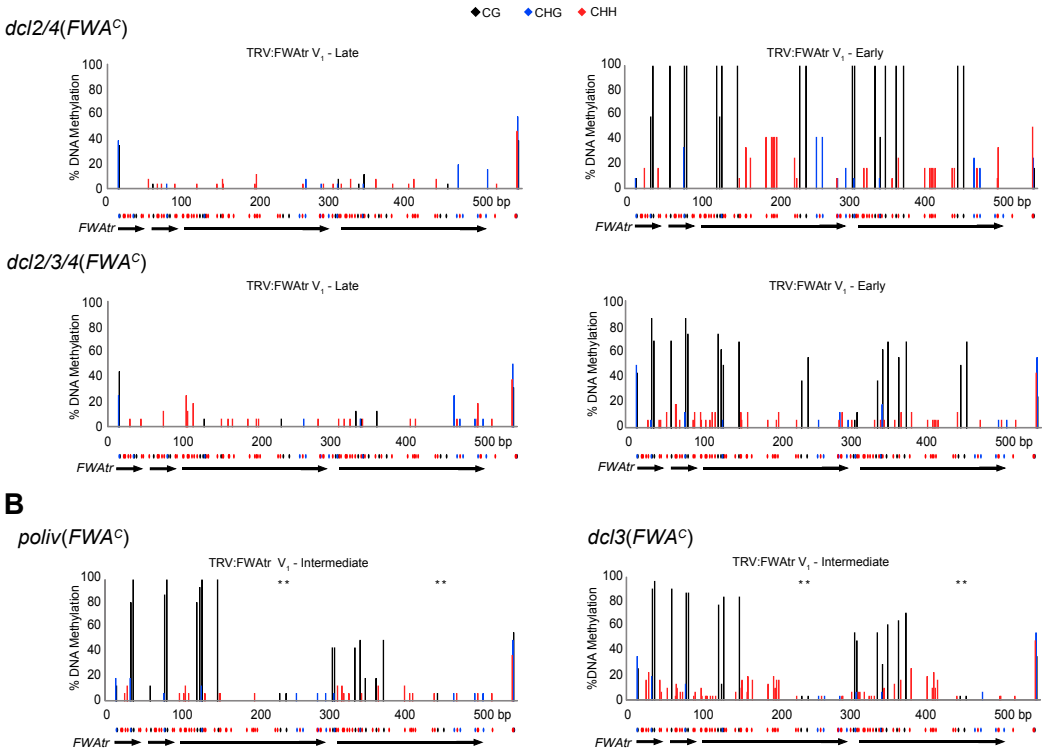

Fig. S6. VIGS of *FWA* establishes CG methylation in RdDM mutants. (*A*) Bisulfite sequencing analysis of DNA methylation at *FWAtr* , in representative late-flowering (left hand side) and early-flowering (right hand side) V_1 progeny of Col-0(*FWA*^{C}), *poliv*(*FWA*^{C}), *rdr2*(*FWA*^{C}), *dcl3*(*FWA*^{C}), *ago4*(*FWA*^{C}), *polv*(*FWA*^{C}), *drm1/2*(*FWA*^{C}), *dcl2/4*(*FWA*^{C}), and *dcl2/3/4*(*FWA*^{C}) plants infected with TRV:FWAtr, TRV, or mock conditions. For *polv*(*FWA*^{C}) and *drm1/2*(*FWA*^{C}) plants, samples from the V_1 progeny of mock-infected plants were assayed because no early-flowering progeny of TRV:FWAtr-infected plants were observed for these genotypes. The position of C residues along the *FWAtr* region is represented by the ticks on the *x* axis and the context of methylation is represented by the different colors: CG is in black, CHG is in blue, and CHH is in red. (*B*) Bisulfite sequencing analysis of DNA methylation at *FWAtr* in representative intermediate-flowering V_1 progeny of *poliv*(*FWA*^{C}) and *dcl3*(*FWA*^{C}) plants infected with TRV:FWAtr. The position of C residues along the *FWAtr* region is represented by the ticks on the *x* axis and the context of methylation is represented by the different colors: CG is in black, CHG is in blue, and CHH is in red. The four CG residues that are actively demethylated in the VN by DME (1, 2) are represented by an asterisk.

1. Calarco JP, et al. (2012) Reprogramming of DNA methylation in pollen guides epigenetic inheritance via small RNA. *Cell* 151(1):194–205.
2. Schoft VK, et al. (2011) Function of the DEMETER DNA glycosylase in the *Arabidopsis thaliana* male gametophyte. *Proc Natl Acad Sci USA* 108(19):8042–8047.

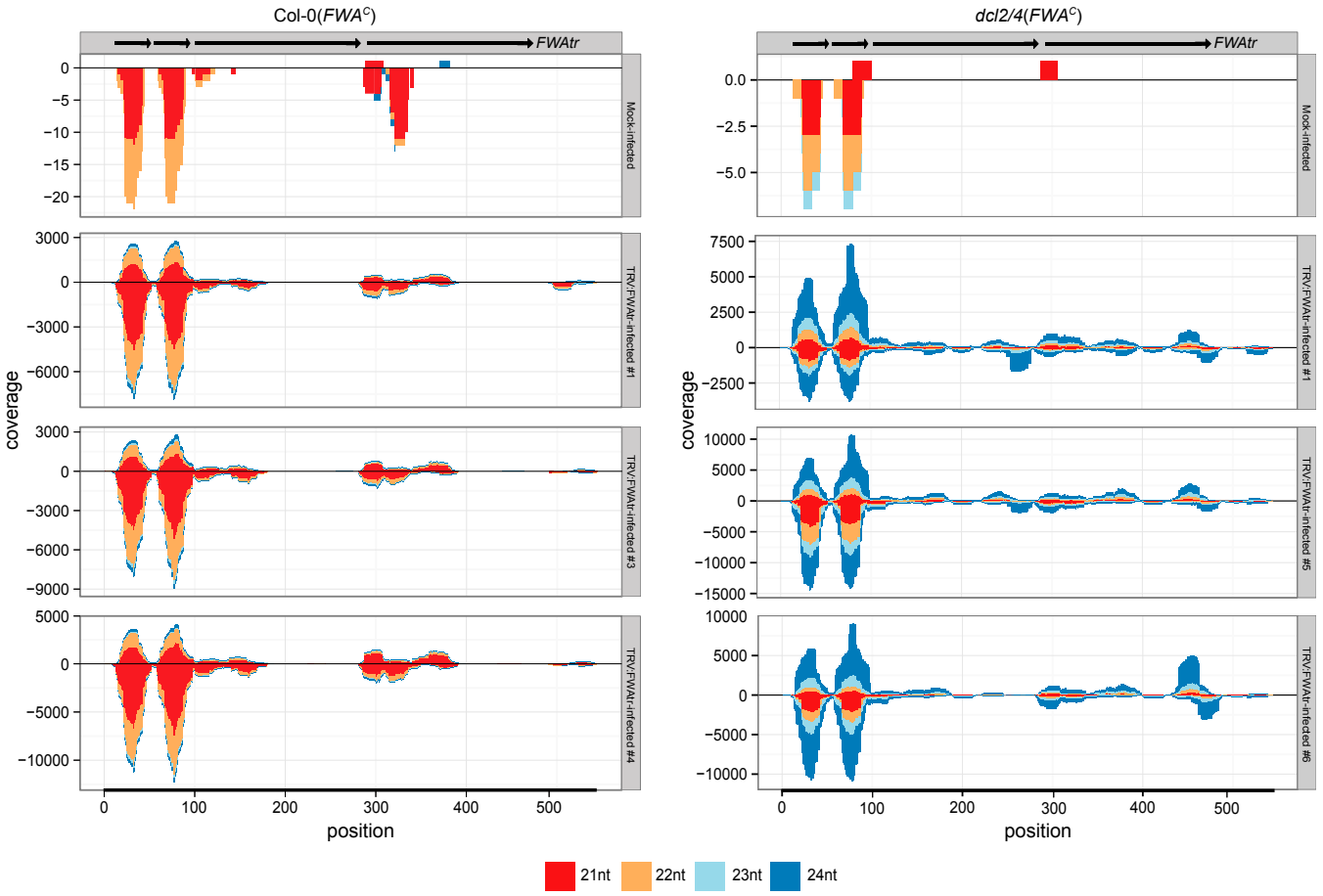

Fig. S7. A high proportion of 21/22 nt sRNAs that map to *FWAtr* are present in the *dcl2/4*(*FWA*^{C}) V_0 plants infected with TRV:FWAtr. The distribution of different size class sRNAs that map to *FWAtr* in mock- and TRV:FWAtr-infected Col-0(*FWA*^{C}) (left hand side) and *dcl2/4*(*FWA*^{C}) (right hand side) V_0 plants. One mock-infected and three TRV:FWAtr-infected RNA samples per genotype were assessed (see Fig. S4 *A* and *C* for the sRNA Northern blot and Northern blot, respectively, with these samples). The distribution includes coverage of 21-nt (red), 22-nt (orange), 23-nt (light blue), and 24-nt (dark blue) sRNAs and includes all possible matches that map to the positive and negative strand of *FWAtr*, normalized to the size of the sRNA library. The *FWAtr* region cloned into TRV is represented by the thick black line on the *x* axis and the position of the tandem repeat (*FWAtr*) is marked at the top of each figure.

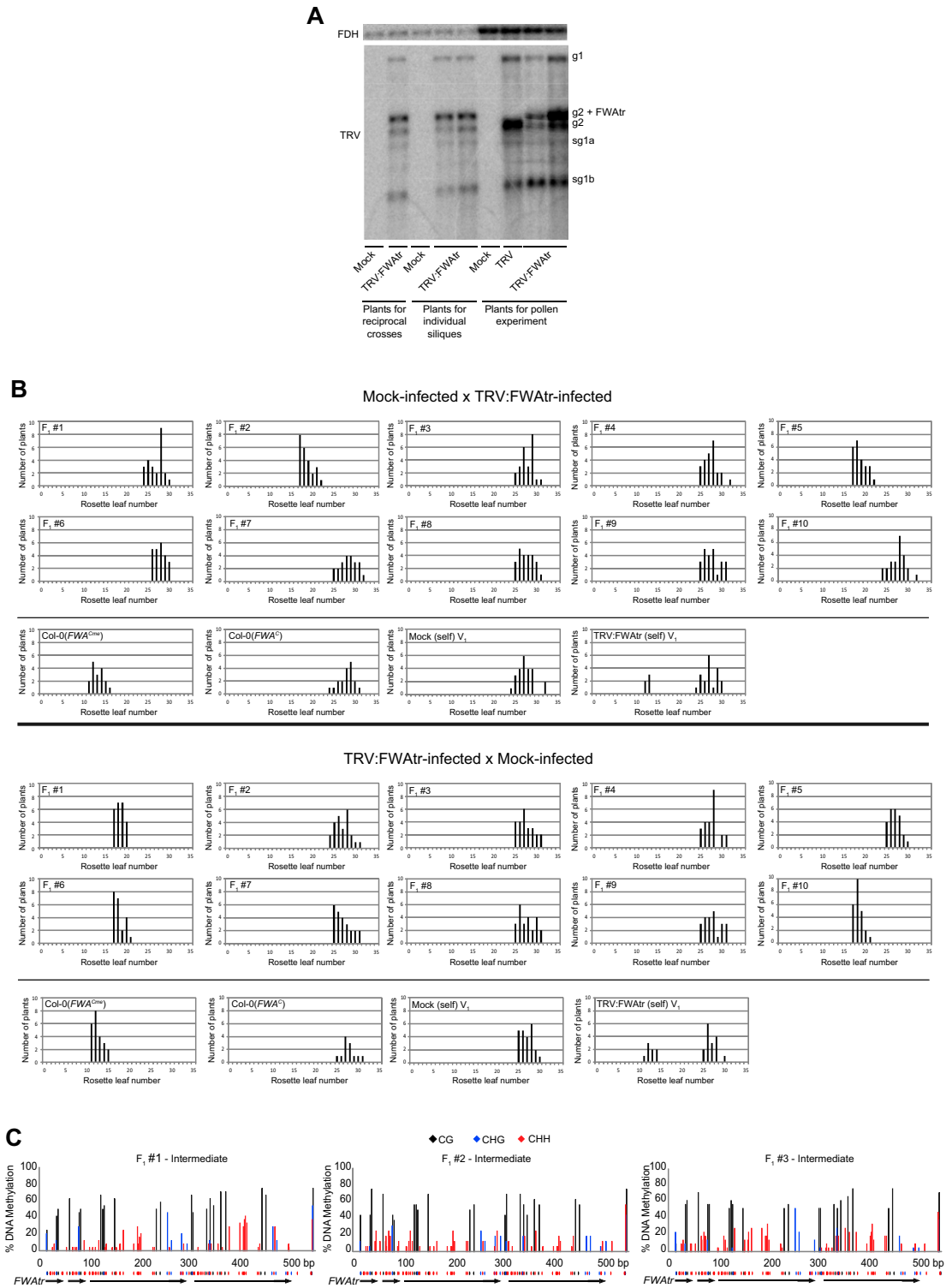

Fig. S8. (Continued)

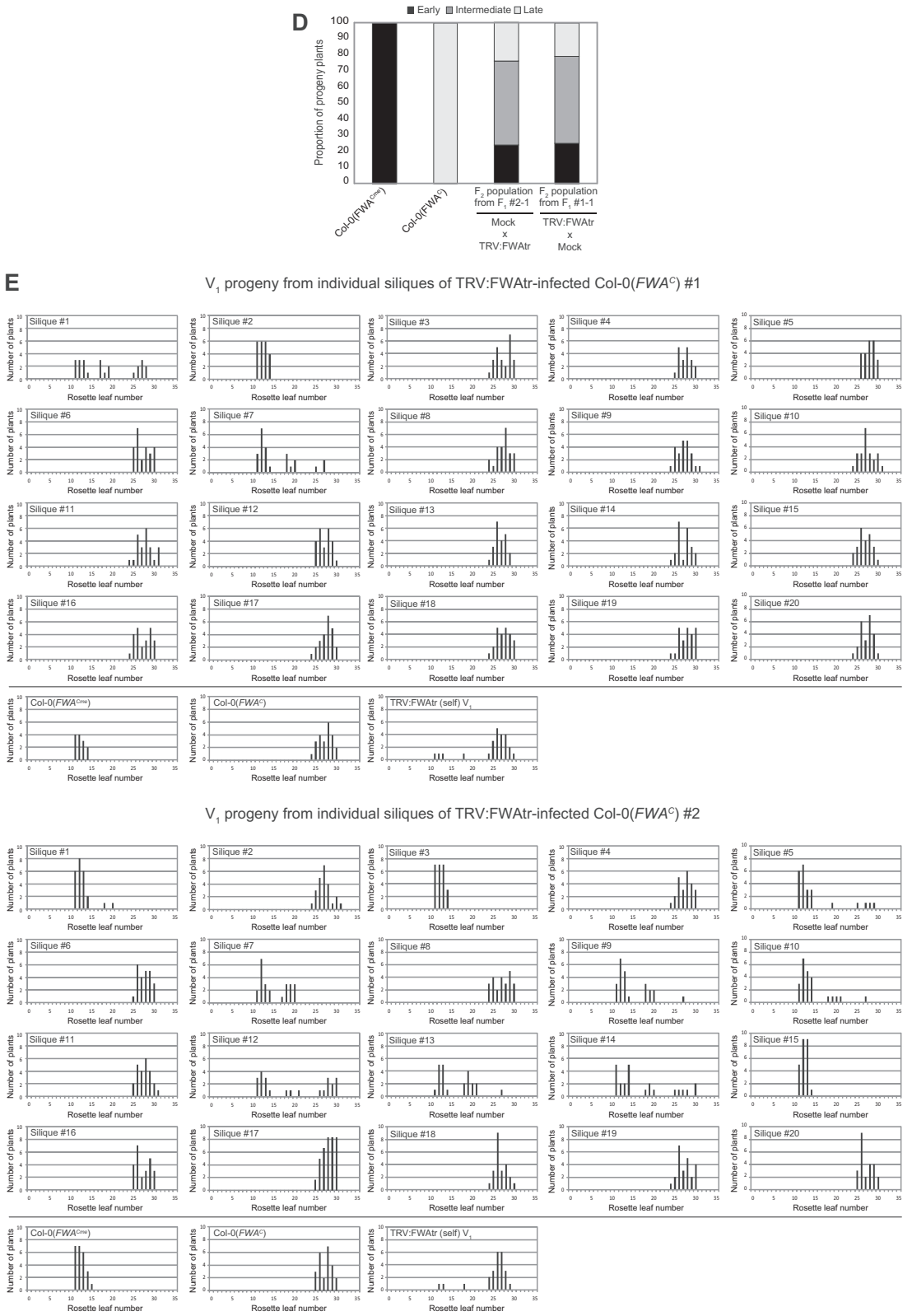

Fig. S8. Heritable DNA methylation at *FWA* is established by VIGS before or during gametogenesis. (*A*) Northern blot analysis of TRV RNA species from leaves of TRV:FWAtr-, TRV-, or mock-infected plants, 14 dpi, used for various experiments to understand when and where DNA methylation is established at *FWA* by VIGS-RdDM. (*Left*) Infected plants used for reciprocal crosses (see F_1 progeny data presented in Fig. 4 *A* and *B*, Fig. S8 *B* and *C*). (*Center*) Infected plants used for testing progeny plants harvested from individual siliques (see *E*). (*Right*) Infected plants used to determine the level of DNA methylation at *FWA* in pollen from TRV:FWAtr-infected Col-0(*FWA*^{C}) plants (see Fig. 5*A* and Fig. S9*A*). *FDH* was probed as a loading control. (*B*) Flowering time (rosette leaf number) of F_1 plants from representative reciprocal crosses between mock-infected and TRV:FWAtr-infected plants. Approximately 24 F_1 plants from 10 different reciprocal crosses

Legend continued on following page

(mock-infected × TRV:FWAtr-infected and TRV:FWAtr-infected × mock-infected) were assayed. Flowering-time data for self-fertilized Col-0(FWA^{C}), Col-0 (FWA^{Cme}), mock-infected and TRV:FWAtr-infected Col-0(FWA^{C}) plants is also presented. (*C*) Bisulfite sequencing analysis of DNA methylation at *FWAtr* in representative F_1 progeny, from reciprocal crosses between mock- and TRV:FWAtr-infected plants, with an intermediate flowering time phenotype. The position of C residues along the *FWAtr* region is represented by the ticks on the *x* axis and the context of methylation is represented by the different colors: CG is in black, CHG is in blue, and CHH is in red. (*D*) Proportion of early- (black), intermediate- (dark gray), and late- (light gray) flowering F_2 plants from two different F_1 plants produced from reciprocal crosses between mock-infected and TRV:FWAtr-infected plants (mock-infected × TRV:FWAtr-infected: #2-1; TRV:FWAtr-infected × mock-infected: #1-1). The total rosette leaf number was measured from ~48 F_2 plants from each population. Flowering time of self-fertilized Col-0(FWA^{Cme}) and Col-0(FWA^{C}) plants are also presented. (*E*) Flowering time (rosette leaf number) of V_1 progeny plants from individual siliques of TRV:FWAtr-infected plants. Approximately 24 plants from 20 individual siliques harvested from two representative TRV:FWAtr-infected plants were assayed. Flowering time data for self-fertilized, pooled seed from Col-0 (FWA^{Cme}), Col-0 (FWA^{C}), and TRV:FWAtr-infected Col-0 (FWA^{C}) plants is also presented.

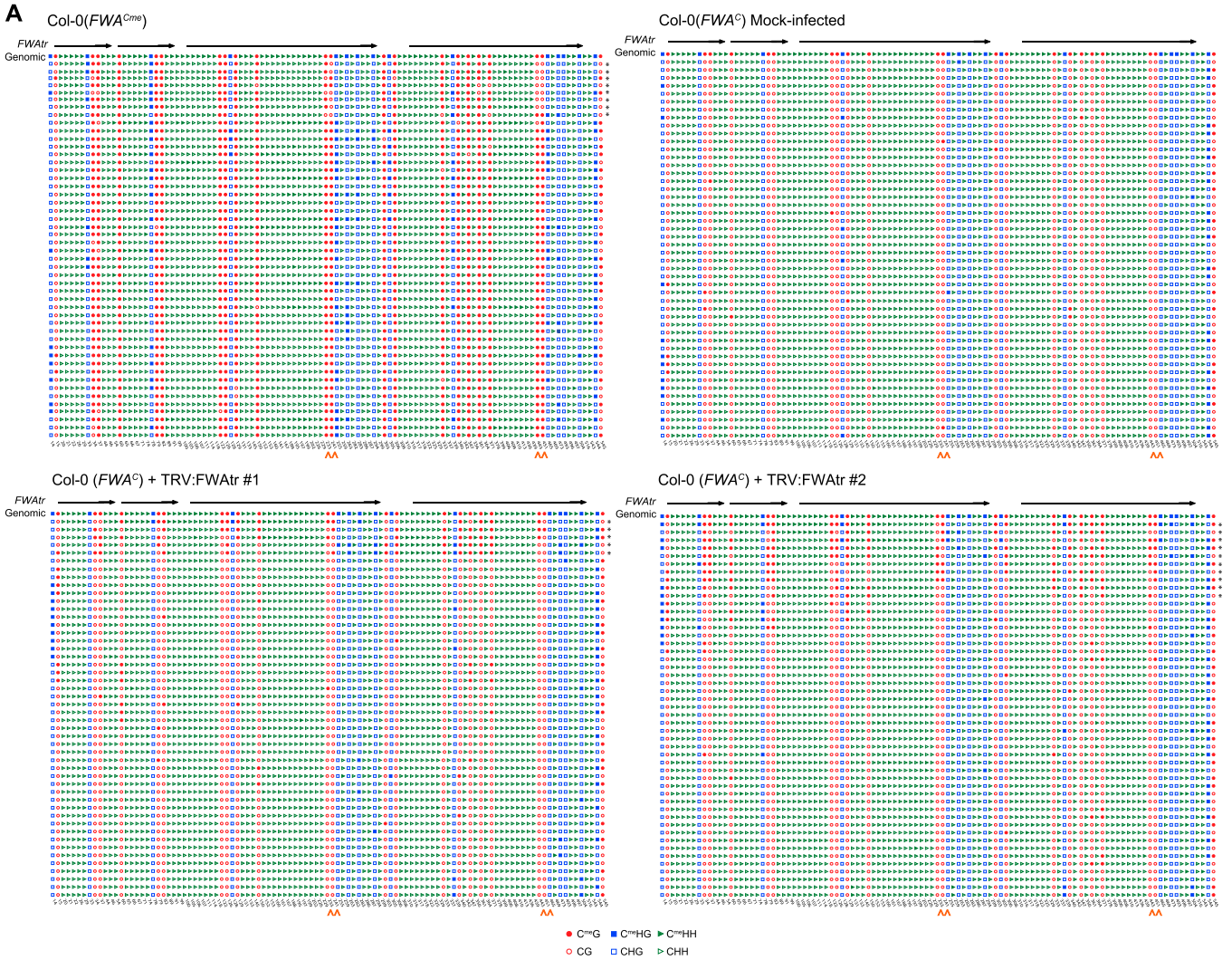

Fig. S9. (Continued)

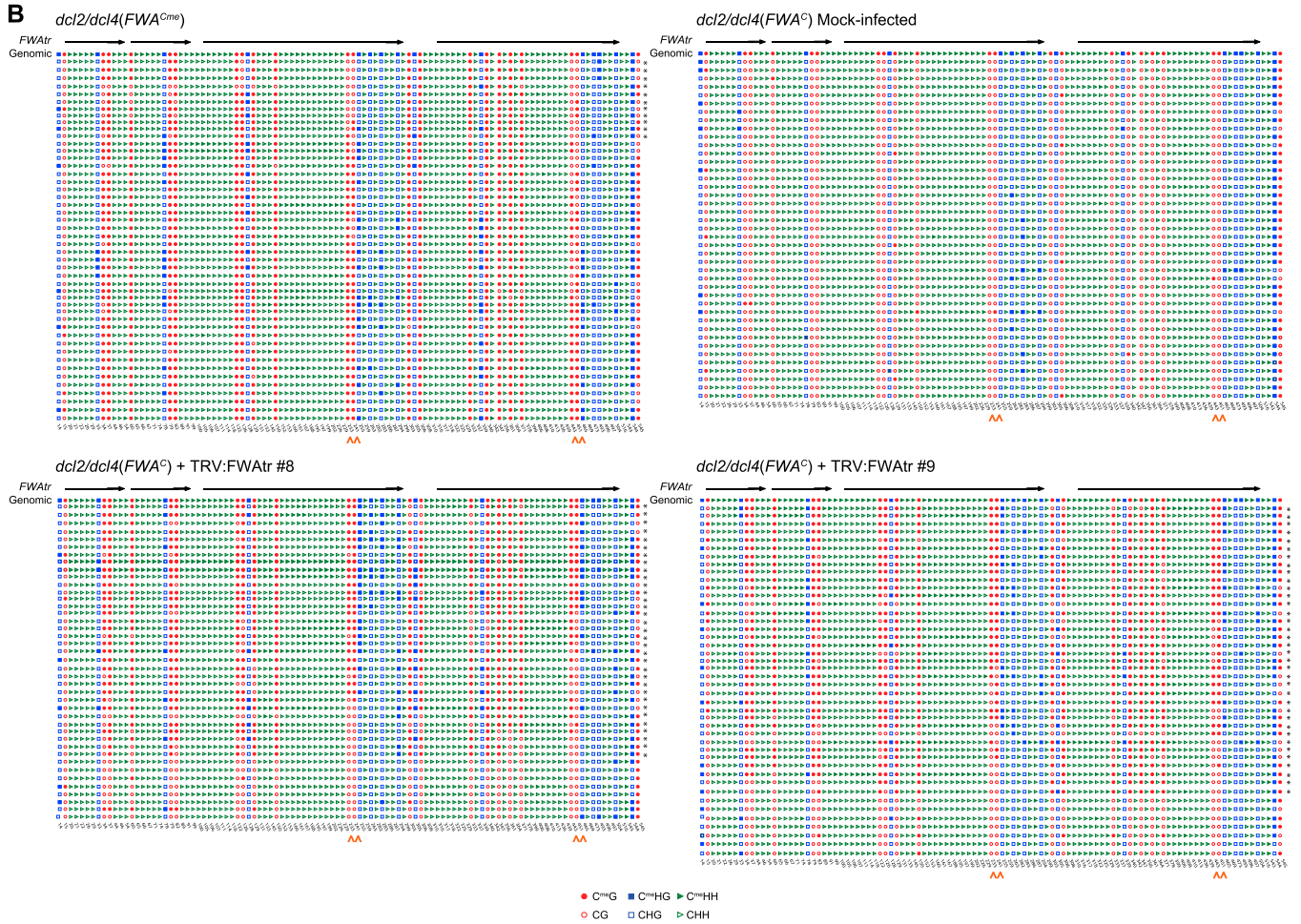

Fig. S9. (Continued)

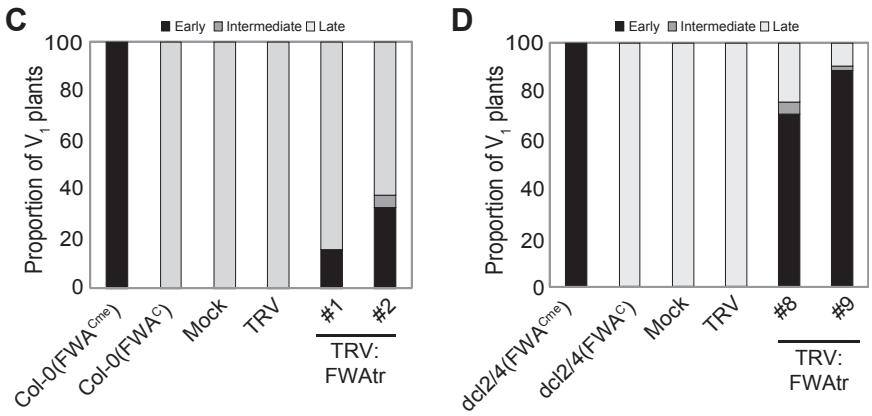

Fig. S9. Pollen DNA from TRV:FWAtr-infected plants is methylated and gives rise to early-flowering progeny. (*A*) Raw bisulfite sequencing data (~48 clones) of DNA methylation at *FWAtr* in pollen DNA from Col-0(*FWA*^{Cme}), mock-infected, and two TRV:FWAtr-infected Col-0(*FWA*^{C}) plants. This figure was generated by CyMate (1) to show the methylation status of each C residue at *FWAtr* within individual clones, representing DNA from either the VN or SC of different pollen grains. Black arrows indicate the position of *FWA* tandem repeats. The position of C residues along the *FWAtr* region analyzed are given at the bottom of each sample. The context of methylation is represented by the different shapes/color: CG is red circles, CHG is blue squares, and CHH is green triangles. Methylated residues are filled and unmethylated residues are not. The C residues that are known to be demethylated in the VN (2, 3) are marked with an orange caret (^). For Col-0(*FWA*^{Cme}), clones that are from the VN are marked with the asterisk. For TRV:FWAtr-infected Col-0(*FWA*^{C}) plants, clones with a high level of methylation are marked with an asterisk. (*B*) Raw bisulfite sequencing data (~48 clones) of DNA methylation at *FWAtr* in pollen DNA from *dcl2/4*(*FWA*^{Cme}), mock-infected, and two TRV:FWAtr-infected *dcl2/4*(*FWA*^{C}) plants. This figure was generated by CyMate (1) to show the methylation status of each C residue at *FWAtr* within individual clones, representing DNA from either the VN or SC of different pollen grains. Black arrows indicate the position of *FWA* tandem repeats. The position of C residues along the *FWAtr* region analyzed are given at the bottom of each sample. The context of methylation is represented by the different shapes/colors: CG is red circles, CHG is blue squares, and CHH is green triangles. Methylated residues are filled and unmethylated residues are not. The C residues that are known to be demethylated in the VN of pollen (2, 3) are marked with an orange caret (^). For *dcl2/4*(*FWA*^{Cme}), clones that are from the VN are marked with the asterisk. For TRV:FWAtr-infected *dcl2/4*(*FWA*^{C}) plants, clones with a high level of methylation are marked with an asterisk. (*C*) Proportion of early- (black), intermediate- (dark gray), and late- (light gray) flowering progeny from TRV:FWAtr-, TRV-, or mock-infected Col-0(*FWA*^{C}) plants. Col-0 (*FWA*^{Cme}) and Col-0(*FWA*^{C}) plants were grown and measured at the same time. The total rosette leaf number was measured from ~48 individual V_1 progeny from each line presented in Fig. 5*A* and Fig. S9*A*. (*D*) Proportion of early- (black), intermediate- (dark gray), and late- (light gray) flowering progeny plants from TRV:FWAtr-, TRV- or mock-infected *dcl2/4*(*FWA*^{C}) plants. *dcl2/4*(*FWA*^{Cme}) and *dcl2/4*(*FWA*^{C}) plants were grown and measured at the same time. The total rosette leaf number was measured from ~48 individual V_1 progeny from each line presented in Fig. 5*B* and Fig. S9*B*.

1. Hetzl J, Foerster AM, Raidl G, Mittelsten Scheid O (2007) CyMATE: A new tool for methylation analysis of plant genomic DNA after bisulphite sequencing. *Plant J* 51(3):526–536.
2. Calarco JP, et al. (2012) Reprogramming of DNA methylation in pollen guides epigenetic inheritance via small RNA. *Cell* 151(1):194–205.
3. Schoft VK, et al. (2011) Function of the DEMETER DNA glycosylase in the *Arabidopsis thaliana* male gametophyte. *Proc Natl Acad Sci USA* 108(19):8042–8047.

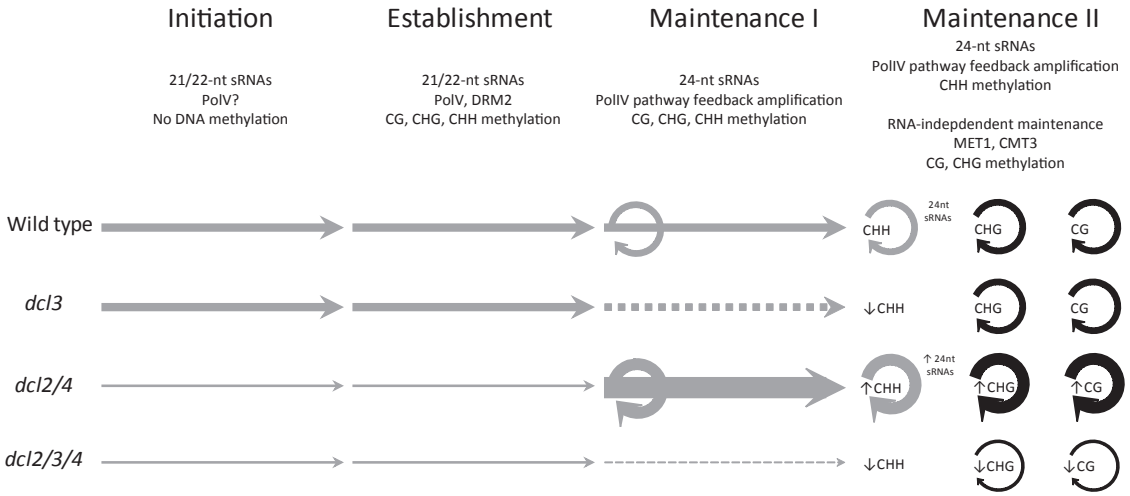

Fig. S10. Model for the establishment of RNA-mediated de novo silencing in *Arabidopsis thaliana* based on VIGS-RdDM at *FWA*. This figure depicts the progressive nature of VIGS-RdDM in wild-type plants compared with various RNA silencing mutants: *dcl3*, defective in 24-nt sRNAs; *dcl2/4*, defective in 21/22-nt sRNAs; and *dcl2/3/4*, defective in 21/22/24-nt sRNAs. On infection, the viral-derived sRNAs (21/22-nt) produced by the antiviral RNA silencing pathway are responsible for the initiation phase of silencing. This is likely to be independent of DNA methylation but requires PolV, and occurs at a similar level in wild-type and *dcl3* plants. However, in a *dcl2/4* and *dcl2/3/4* mutant the 21/22-nt viral sRNAs are reduced and results in a lower level of the initiation phase. Once the correct chromatin environment is established, the 21/22-nt sRNAs can recruit the de novo methyltransferase DRM2 to the target site to catalyze and establish DNA methylation in all sequence contexts. Once established in wild-type, CG, CHG, and CHH methylation can be reinforced and maintained by 24-nt sRNAs produced by the PolIV pathway feedback amplification (Maintenance I). However, PolIV-RdDM reinforcement of CHH methylation is not essential as CG and CHG methylation can continue to be established in a *dcl3* mutant by the 21/22-nt viral sRNAs, and then it can be maintained by the RNA-independent maintenance mechanisms (Maintenance II). In contrast, the low level of initiation in a *dcl2/4* mutant will lead to a low level of establishment of DNA methylation. This can be overcome by the action of DCL3 that produces 24-nt sRNAs, which results in amplification of DNA methylation in all sequence contexts via the PolIV-RdDM feedback mechanism. As such, there will be overall higher levels of CG, CHG, and CHH methylation at the target locus that can be maintained by the RNA-independent and 24-nt sRNA-dependent (PolIV-RdDM) maintenance mechanisms. This effect is completely abolished in a *dcl2/3/4* mutant because of the lack of 24-nt sRNAs and thus amplification and reinforcement by PolIV-RdDM. This means only the low level of symmetric DNA methylation (CG and CHG) established by the 21/22-nt viral sRNAs during the establishment phase will be maintained by MET1 and CMT3. ↑ represents increase, relative to wild type; ↓ represents decrease, relative to wild-type. Gray horizontal arrows represent the progression of RNA-mediated de novo silencing. Gray circular arrows represent the self-reinforcing CHH methylation maintenance loop mediated by 24-nt sRNAs. Dashed line represents the bypassing of Maintenance I, which progresses independent of DCL3. Black circular arrows represent the RNA-independent DNA methylation self-reinforcing maintenance loops for CG (mediated by MET1) and CHG (mediated by CMT3) contexts. The thicker the arrow, the stronger the effect at each phase of RNA-mediated de novo silencing.

Table S1. RNA silencing mutants introgressed into the *fwa-d* epimutant

Mutant	Line	Gene	AGI	Mutation	Source
poliv	*nrpd1a-4*	*NRPD1*	At1g63020	T-DNA (SALK_083051)	(1)
rdr2	*rdr2-2*	*RDR2*	At4g11130	T-DNA (SALK_059661)	(2)
dcl3	*dcl3-1*	*DCL3*	At3g43920	T-DNA (SALK_005512)	(3)
ago4	*ago4-3*	*AGO4*	At2g27040	T-DNA (WISC_338A06)	(4)
polv	*nrpe1-1*	*NRPE1*	At2g40030	EMS	(5)
drm1/2	*drm1-2/drm2-2*	*DRM1*	At5g15380	T-DNA (SALK_031705) x	(6)
		DRM2	At5g14620	T-DNA (SALK_150863)	
dcl2/4	*dcl2-1/dcl4-2*	*DCL2*	At3g03300	T-DNA (SALK_064627) x	(7)
		DCL4	At5g20320	T-DNA (GABI_160G05)	
dcl2/3/4	*dcl2-1/dcl3-1/dcl4-2*	*DCL2*	At3g03300	T-DNA (SALK_064627) x	(8)
		DCL3	At3g43920	T-DNA (SALK_005512) x	
		DCL4	At5g20320	T-DNA (GABI_160G05)	
dcl2	*dcl2-1*	*DCL2*	At3g03300	T-DNA (SALK_064627)	(3)
dcl4	*dcl4-2*	*DCL4*	At5g20320	T-DNA (GABI_160G05)	(9)

1. Pontier D, et al. (2005) Reinforcement of silencing at transposons and highly repeated sequences requires the concerted action of two distinct RNA polymerases IV in *Arabidopsis*. *Genes Dev* 19(17):2030–2040.
2. Vazquez F, et al. (2004) Endogenous trans-acting siRNAs regulate the accumulation of *Arabidopsis* mRNAs. *Mol Cell* 16(1):69–79.
3. Xie Z, et al. (2004) Genetic and functional diversification of small RNA pathways in plants. *PLoS Biol* 2(5):E104.
4. Havecker ER, et al. (2010) The *Arabidopsis* RNA-directed DNA methylation argonautes functionally diverge based on their expression and interaction with target loci. *Plant Cell* 22(2):321–334.
5. Kanno T, et al. (2005) Atypical RNA polymerase subunits required for RNA-directed DNA methylation. *Nat Genet* 37(7):761–765.
6. Chan SW-L, et al. (2006) RNAi, DRD1, and histone methylation actively target developmentally important non-CG DNA methylation in *Arabidopsis*. *PLoS Genet* 2(6):e83.
7. Deleris A, et al. (2006) Hierarchical action and inhibition of plant Dicer-like proteins in antiviral defense. *Science* 313(5783):68–71.
8. Henderson IR, et al. (2006) Dissecting *Arabidopsis thaliana* DICER function in small RNA processing, gene silencing and DNA methylation patterning. *Nat Genet* 38(6):721–725.
9. Xie Z, Allen E, Wilken A, Carrington JC (2005) DICER-LIKE 4 functions in trans-acting small interfering RNA biogenesis and vegetative phase change in *Arabidopsis thaliana*. *Proc Natl Acad Sci USA* 102(36):12984–12989.

Table S2. Oligonucleotides used in the present study

Oligonucleotide	Sequence
Viral clones	
FWAtr forward	CCGGATCCGAGTTATGGGCCGAAGCCC
FWAtr reverse (XhoI)	GGCTCGAGTCGGGAACCAAAATCATTCTC
FWAtr reverse (BamHI)	CCGGATCCTCGGGAACCAAAATCATTCTC
FWAcds forward	CCGGATCCGTGGTAAGGCAACTAATTGTGGAG
FWAcds reverse (XhoI)	GGCTCGAGGTGTCCATAAGAGTCTTGACCAGAGTC
FWAcds reverse (BamHI)	CCGGATCCGTGTCCATAAGAGTCTTGACCAGAGTC
qPCR, RT-PCR, and OneStep qPCR	
FWA RT forward (1)	GCTCACTCCAACAGATTCAAGCAG
FWA RT reverse (1)	GTTGGTAGATGAAAGGGTCGAGAG
FDH forward	TTGGACTTGCTGTTGCCGA
FDH reverse	AAGTTCCCCATCCCTTGTGAC
TRV forward	TCTGTTTCTGTGTATAGACTGTTTGAG
TRV reverse	GTAATAACGCTTACGTAGGCGAG
TRV backbone forward[#]	TGTTCAGGCGGTTCTTGTGTGTC
TRV:FWAcds reverse[Δ]	GGCTCGAGGTGTCCATAAGAGTCTTGACCAGAGTC
TRV:FWAtr reverse*	GCTCGTATGAATGTTGAATGGGATAAGG
McrBC assay	
FWA McrBC forward (2)	GCCATTGGTCCAAGTGCTAT
FWA McrBC reverse (2)	CGGTGCTCGTATGAATGTTG
Bisulfite sequencing	
FWA bisulfite forward (3)	GGTTTTATATTAATATTAAAGAGTTATGGGTYGAAGTTT
FWA bisulfite reverse (3)	CAAAATACTTTACACATAAACRAAAAACAAACAAATCRAA
FWA nested forward (1)	AAAGAGTTATGGGYYGAAG
FWA nested reverse (1)	CRRRAACCAAAATCATTCTCTAAACA
FWA bisulfite forward - pollen	ATTAAAGAGTTATGGGYYGAAGTTTAT
FWA bisulfite reverse - pollen	CRRRAACCAAAATCATTCTCTAAACA
PCR products for radioactive probes	
FWAtr forward	CCGGATCCGAGTTATGGGCCGAAGCCC
FWAtr reverse (XhoI)	GGCTCGAGTCGGGAACCAAAATCATTCTC
FWAcds forward	CCGGATCCGTGGTAAGGCAACTAATTGTGGAG
FWAcds reverse (XhoI)	GGCTCGAGGTGTCCATAAGAGTCTTGACCAGAGTC
FDH forward	TTGGACTTGCTGTTGCCGA
FDH reverse	AAGTTCCCCATCCCTTGTGAC
Olionucleotide probes	
U6	GCTAATCTTCTCTGTATCGTTCC
AtRep2	GCGGGACGGGTTTGGCAGGACGTTACTTAAT

Restriction sites used for cloning are underlined. References of previously published oligos are given. To test level of TRV:FWAtr, use primers marked # and Δ; for TRV:FWAcds use primers marked # and *.

1. Kinoshita Y, et al. (2007) Control of FWA gene silencing in *Arabidopsis thaliana* by SINE-related direct repeats. *Plant J* 49(1):38–45.
2. Johannes F, et al. (2009) Assessing the impact of transgenerational epigenetic variation on complex traits. *PLoS Genet* 5(6):e1000530.
3. Chan SW-L, Zhang X, Bernatavichute YV, Jacobsen SE (2006) Two-step recruitment of RNA-directed DNA methylation to tandem repeats. *PLoS Biol* 4(11):e363.